Assessment of Resistance in Wild Barley Genotypes to Fusarium Head Blight under Single and Co-infection Conditions

Mohsin Bashir Khan

Independent Project in Biology, A2E • 30 credits
Swedish University of Agricultural Sciences, SLU
Department of Forest Mycology and Plant Pathology
Plant Biology for Sustainable Production - Master's Programme - Abiotic and Biotic Interactions of Cultivated Plants – LM011
Uppsala, 2026



Assessment of Resistance in Wild Barley Genotypes to Fusarium Head Blight under Single and Co-infection Conditions

Mohsin Bashir Khan

Supervisor:	**Vahidehalsadat Rafieebanadaki, Department of Forest Mycology and Plant Pathology, SLU**
Assistant supervisor:	Fredrik Dolfors, Department of Forest Mycology and Plant Pathology, SLU
Assistant supervisor:	Magnus Karlsson, Department of Forest Mycology and Plant Pathology, SLU
Examiner:	Anna Berlin, Department of Forest Mycology and Plant Pathology, SLU

Credits:	30 credits
Level:	Second cycle (A2E)
Course title:	Independent Project in Biology, A2E
Course code:	EX0856
Programme/education:	Plant Biology for Sustainable Production – Master's Programme
Course coordinating dept:	Department of Plant Biology
Place of publication:	Uppsala
Year of publication:	2026

Keywords:	*Fusarium* species complex, wild barley, *Hordeum vulgare subsp. spontaneum,* disease resistance, high-throughput phenotyping, trichothecene biosynthesis genes

Swedish University of Agricultural Sciences

Faculty of Natural Resources and Agricultural Sciences

Department of Forest Mycology and Plant Pathology

Abstract

Fusarium head blight (FHB) is a major fungal disease and a serious threat to food and feed safety around the globe. It primarily affects small-grain cereals, reducing yield and contaminating grain with mycotoxins. The polygenic and quantitative nature of FHB resistance in cultivated barley (*Hordeum vulgare*) is a major bottleneck for durable resistance. This study evaluated FHB resistance in a diverse panel of wild barley (*Hordeum vulgare subsp. spontaneum*) genotypes from the Wild Barley Diversity Collection (WBDC) using a detached leaf assay under three treatments: uninoculated control, single-species infection with *Fusarium graminearum*, and mixed-species co-infection with three species: *F. graminearum*, *F. avenaceum*, and *F. culmorum*. Disease severity was assessed using two complementary phenotyping approaches: conventional visual disease scoring and image-based lesion quantification using ImageJ. Both methods revealed a highly significant effect of treatment on disease severity, substantial genotypic variation in susceptibility, and a significant genotype-by-treatment interaction, indicating that the relative ranking of genotypes shifted depending on infection type. Several genotypes showed consistent low and high disease indices across both scoring methods. WBDC-110 and WBDC-164 were among the most susceptible genotypes with both methods, whereas WBDC-060, WBDC-034 and WBDC-120 were the three least susceptible, suggesting partial resistance worth further characterisation. Co-infection did not affect all genotypes in the same way: it increased disease in some genotypes but reduced it in WBDC-110 and WBDC-164, the genotypes most damaged by *F. graminearum* alone. Molecular assays were also used to complement the phenotypic data. In two contrasting genotypes, WBDC-060 and WBDC-159, the *F. graminearum*-specific FG16N PCR assay detected the pathogen in single-species infected leaves but not in co-infected leaves. In contrast, a deoxynivalenol (DON)-type Tri13 sequence was detected only in co-infected samples, and no nivalenol (NIV)-type sequence was detected in any sample. These results suggest that co-infection changes the composition of the fungal community in the leaf, possibly through competition with *F. graminearum*, and that the DON-type signal in co-infected leaves may come from *F. culmorum*; quantitative methods are needed to test these explanations. These findings highlight the value of combining phenotypic and molecular approaches when characterising FHB resistance, and point to wild barley genotypes such as WBDC-060 as promising candidates for further resistance breeding and mechanistic study.

Keywords: *Fusarium* species complex, wild barley, *Hordeum vulgare subsp. spontaneum,* disease resistance, high-throughput phenotyping, trichothecene biosynthesis genes

Contents

1. Introduction 8
1.1 Fusarium head blight: a major threat to cereal production 8
1.2 The *Fusarium* species complex and co-infection in cereals 9
1.3 Barley and the challenges of FHB management 10
1.4 Resistance to Fusarium head blight in barley 10
1.5 Wild barley as a source of novel resistance 11
1.6 Phenotyping approaches for evaluating FHB resistance 12
1.7 The detached leaf assay as a rapid phenotyping tool 13
1.8 Knowledge gaps and rationale 14
1.9 Aim and objectives 15

2. Materials and Methods 16
2.1 Plant material 16
2.2 Plant growth conditions 16
2.3 Fungal isolates and inoculum preparation 17
2.3.1 Spore harvesting 18
2.3.2 Spore counting 18
2.4 Detached leaf assay 19
2.4.1 Experimental design, biological and technical replication 19
2.4.2 Leaf preparation and placement 19
2.5 Disease assessment and digital image analysis 20
2.5.1 Digital imaging 21
2.5.2 Disease scoring and visual assessment 21
2.5.3 Image-based lesion quantification 22
2.5.4 Data processing and statistical analysis 23
2.5.5 Repeat trial and selection of genotypes for molecular analysis 24
2.6 DNA extraction 25
2.7 PCR reagents and amplification conditions 25
2.7.1 Detection of trichothecene biosynthesis genes (DON and NIV primers) 26
2.7.2 Agarose gel electrophoresis and PCR product visualization 27

3. Results 28
3.1 Phenotypic analysis based on visual scoring 28
3.2 Phenotypic analysis 31
3.3 PCR detection of *F. graminearum* and Tri13 sequences 35

4. Discussion 38
4.1 Limitations 40
4.2 Implications and future work 41

5. Conclusions 43

References 44

Popular science summary **48**

Acknowledgements **49**

Appendix 1 ..... **50**

List of Tables

Table 1. Two-way ANOVA for Disease Index (visual scoring) 28

Table 2. Pairwise comparisons of treatments based on estimated marginal means using Tukey's post-hoc test (visual scoring) 29

Table 3. Most and least susceptible genotypes (visual scoring) 29

Table 4. Two-way ANOVA for Disease Index (ImageJ-based quantification, log2-transformed) 32

Table 5. Pairwise comparisons of treatments based on estimated marginal means using Tukey's post-hoc test (log2 scale) 32

Table 6. Most and least susceptible genotypes (ImageJ-based quantification; mean $\log_2(DI + 1)$ across treatments) 33

Table 7. Co-infection effect for selected genotypes: mean lesion area (mm^2, untransformed) under each treatment and the difference between Mix infection and F. graminearum alone (ImageJ quantification) 33

List of Figures

Figure 1. Barley genotypes cultivated in the greenhouse 17

Figure 2. Preparing fungal mycelia and inoculum for screening barley genotypes 18

Figure 3. Counting and adjusting the spores of Fusarium species on a hemocytometer 19

Figure 4. Detached leaf assay and inoculation of barley leaves with Fusarium species 20

Figure 5. Incubation of inoculated detached leaves of different barley genotypes in the growth chambers at different time points 21

Figure 6. Digital imaging of lesion size of inoculated leaves for each treatment and genotype 21

Figure 7. Disease scoring scale from 0 to 8 corresponding to the level of severity and lesion size caused by Fusarium infection that was used as a reference for visual disease assessment 22

Figure 8. Measurement of lesion area in ImageJ: calibration of the image scale (left) and manual delineation of the necrotic lesion, excluding the chlorotic halo (right) 23

Figure 9. Representative lesion development in the susceptible genotype WBDC-10 (upper panel) and the less susceptible genotype WBDC-18 (lower panel) under single and co-infection treatments 24

Figure 10. Disease index (mean visual score per Petri dish, 0–8 scale) of individual genotypes under control, single infection, and mixed infection conditions.....30

Figure 11. Overall susceptibility of genotypes based on mean disease index averaged across all treatments (visual scoring). Higher values indicate greater susceptibility (0 = no symptoms, 8 = most severe).....30

Figure 12. Overall susceptibility of genotypes based on mean log2(DiseaseIndex + 1) averaged across all treatments (ImageJ). Higher values indicate greater susceptibility.....34

Figure 13. Mean log2(DiseaseIndex + 1) by genotype and treatment, with asterisks denoting Tukey-adjusted significance.....34

Figure 14. Mean ImageJ disease index (lesion area) under single-species inoculation with F. graminearum and mixed-species inoculation (Mix) for each genotype; the difference between the two treatments is the co-infection effect (Section 2.5.4; Table 7).....35

Figure 15. PCR detection of Fusarium graminearum DNA (FG16N assay) in WBDC-060 and WBDC-159 under the F. graminearum (Fg) and co-infection (Mix) treatments. Lane labels give the treatment, genotype and biological replicate (R); L = 1 kb DNA ladder 36

Figure 16. PCR screening for DON-associated (left) and NIV-associated (right) Tri13 sequences in WBDC-060 and WBDC-159 under the F. graminearum (Fg) and co-infection (Mix) treatments. Lane labels give the treatment, genotype and biological replicate (R); L = 1 kb DNA ladder.....37

1. Introduction

Fusarium head blight (FHB) is one of the most economically important diseases of cereal crops throughout the world, with wheat and barley being the prime target. Cereal growing regions around the globe have witnessed FHB epidemics (Dean et al. 2012; McMullen et al. 2012) with devastating social and economic impacts, causing billions of dollars in direct losses to grain yield. The secondary impacts to associated agri-businesses are estimated to be twice the amount of direct losses (Nganje et al. 2004). FHB also comes with serious health risks, since *Fusarium* species are capable of producing a range of mycotoxins, mainly trichothecenes but also oestrogenic mycotoxins such as zearalenone (O'Donnell et al., 2000; Stępień & Chełkowski, 2010). These toxins coupled with reduced weight and functional qualities of seed because of premature development in the form of shrivelled and soft kernels (Trail 2009), render the grain unfit for human and animal consumption, including malting. This chapter describes FHB and its causal species complex, the importance of barley and the limitations of current resistance. Finally we will discuss wild barley as a source of novel resistance and the phenotyping methods available to evaluate it, and end with the knowledge gaps that motivated this study and its aim and objectives.

1.1 Fusarium head blight: a major threat to cereal production

Initially, FHB was considered to be a periodic occurrence contained in a localized area. After 1884 when the disease made its appearance in England and swept across North America in successive outbreaks in wheat and barley crops in the 1990s, this disease became a serious threat to cereal production. During this period, the plant pathologists considered FHB to be a "re-emerging disease of devastating impact" (McMullen et al., 2012), which has become massively significant over the past decades and continues to cause similar losses in cereal growing regions around the world (McMullen et al., 2012). In fields severely affected by FHB, yield reductions of up to 74% have been recorded, shown by inoculation trials (McMullen et al., 2012; Parry et al., 1995). While secondary losses in associated agri-businesses such as grain handling, malting and export losses have been estimated to be about twice the direct losses (Nganje et al. 2004). Some of the reasons why FHB has been bred for on a scale more commonly associated with diseases with much wider host range and has received the same level of research is that the losses are sudden rather than a consistent, predictable decline (McMullen et al., 2012; Parry et al., 1995). A second, quite separate facet

of the danger is that even if the loss of grain is relatively low, *Fusarium* species that infect cereal heads can produce a variety of mycotoxins (Clear et al., 2006; Stanisz et al., 2015) that render the toxic grains unfit for human and animal consumption or malting. As the toxins are stored within the grain, and infected kernels are often shrivelled and physiologically immature (Trail 2009). The quality aspect of FHB damage is not an extra to the yield aspect, as regulatory tolerances for DON in food and feed are very low. A batch of grain may be rejected as inedible or unsuitable for animal feed due to the presence of the mycotoxins- even if the yield or appearance are acceptable. The combination of substantial yield losses, mycotoxin contamination, and the potential for widespread epidemics makes FHB one of the most important diseases of cereal crops around the world. *Fusarium graminearum*, a major causal agent of FHB, is ranked among the ten most scientifically and economically important fungal plant pathogens (Dean et al. 2012). Overall, these effects make FHB a persistent threat to cereal production and reinforce its significance for global food and feed security, particularly in major cereal-growing regions.

1.2 The *Fusarium* species complex and co-infection in cereals

FHB is a disease of a complex nature, the prevalence of which differs with climate and from region to region, and is caused by an interplay of multiple *Fusarium* species. *F. graminearum* is the predominant causal species. In Europe *F. graminearum, F. culmorum* and *F. avenaceum* are consistently reported as among the most important members of the complex, together with *F. poae* (Parry et al., 1995; Pereyra & Dill-Macky, 2010). It is now well known that several of these species are often found together in the same field, and even within the heads or plants (Siou et al. 2015). The interaction between these co-occurring species during infection is partially understood, and much of the available experimental evidence has been generated in wheat. Xu et al. (2007), for example, inoculated wheat with combinations of *Fusarium* species as well as single species and observed that the combinations, depending on the reaction of the species and environmental conditions during the inoculations, affected *Fusarium* development, fungal growth and production of mycotoxins in comparison to single-species inoculations. Subsequent studies in wheat have further demonstrated the complexity of these interactions. (Siou et al. 2015) investigated interactions between *F. graminearum* and other members of the head blight complex using single and pairwise inoculations on wheat spikes under greenhouse and field conditions. The response to co-infection varied among isolates and appeared to depend more strongly on isolate aggressiveness. Ecologically, the co-occurrence of *Fusarium* species has been described as a combination of competitive, and sometimes, synergistic interactions for colonising a host plant. In

wheat, co-inoculation of *F. graminearum* and the weakly pathogenic *F. poae* resulted in reduced symptom development compared with *F. graminearum* alone, while pre-inoculation with *F. poae* prior to *F. graminearum* infection further reduced disease symptoms, *F. graminearum* biomass, and mycotoxin accumulation (Tan et al., 2020). Consequently, field performance under natural, multi-species, disease pressure may not be given as completely as it can be under single species conditions, due to the fact that the response of the host to different species may differ widely, and that the overall response cannot be determined by simply adding the individual responses of the single species.

1.3 Barley and the challenges of FHB management

Barley (*Hordeum vulgare*) is the fourth most widely grown cereal crop globally and is among the few cereals that can withstand a wide variety of climatic conditions, ranging from semi-arid to short season, high latitude environments. Harvest of barley takes place on about 50 million hectares, and the crop is used as a feed for livestock, in malting and brewing industry, and in many parts of the world, as food for humans, a source of fiber, protein and minerals (Zhou, 2010). Barley and wheat are the two cereals most severely affected by FHB (Fernando et al. 2021). Brown, water-soaked lesions are normally seen on spikelets, and under favourable conditions can cover the entire head, causing yield loss, grain quality degradation and mycotoxin contamination. In practice, control of the disease is challenging: the effectiveness of fungicides in the *Fusarium* complex is limited, the timing of sprays around the small flowering window is logistically difficult and the populations of cereal pathogens may also be becoming increasingly resistant to fungicides. Sources of high levels of resistance in cultivated barley are limited, especially for the six-rowed malting types, and none of the resistance available is strong enough to ensure that deoxynivalenol contamination in malting barley is reliably kept below the limits set by the malting and brewing industry in the long term (Ma et al., 2000). Under the influence of climate change, epidemic projections estimate increase in the frequency and severity of FHB with likely increase in the risk of mycotoxin contamination (Madgwick et al., 2011) and spread of the disease into areas where it has not occurred traditionally. Resistance-based solutions are therefore seen as a priority for cereal breeding programmes to sustainably deal with future epidemics.

1.4 Resistance to Fusarium head blight in barley

As in wheat, FHB resistance in barley is a complex, quantitative trait and numerous quantitative trait loci (QTL) have been identified throughout all seven barley chromosomes, many of which have a relatively weak, environment-dependent effect, while only a small number have been found to be consistently

effective across populations and testing environments (Hoheneder et al. 2022). Wheat resistance has been traditionally divided into two types, Type I (resistance to initial infection) and Type II (resistance to the internal growth of the fungus within the head after infection has occurred); similar component-based approaches to resistance have been developed for barley, but the specific wheat and barley resistance components are not the same (Baek et al. 2022). Two of the better characterized barley FHB QTL are on chromosome 2H (bin 8) and 6H (bin 7) and near-isogenic lines with these alleles have provided increased and prompt response to the fungal inoculation with *F. graminearum* compared to their susceptible recurrent parents (Ma et al., 2000). Despite this progress, the mechanisms of quantitative FHB resistance in barley are still poorly understood and introgression of major-effect QTL, like those from the resistant six-rowed cultivar Chevron, has often yielded a very modest resistance phenotype even in elite, agronomically adapted backgrounds (Linkmeyer et al. 2013), which suggests that there is additional resistance provided by other, as yet unidentified, contributing loci and that resistance also depends on genetic background.

1.5 Wild barley as a source of novel resistance

Because resistance to FHB is polygenic and quantitatively inherited, conventional breeding for resistance is slow and difficult to achieve because it involves various genes, each with small effect, influencing resistance rather than one dominant gene that can be easily introgressed. The cultivated barley has undergone several genetic bottlenecks during domestication and subsequent selective breeding, resulting in a lack of allelic diversity within the cultivated barley, compared with the wild barley, when considering many disease resistance traits (Dawson et al. 2015). Wild barley (*Hordeum vulgare* subsp. *spontaneum*) has been repeatedly identified as a rich source of resistance alleles that remain largely underutilized. This diversity was brought together in a manageable and well characterized form by the collection of a number of accessions of wild barley collected primarily from the Fertile Crescent and representatives from Central Asia, North Africa and the Caucasus (Steffenson et al., 2007; Sato et al., 2014) that make up the Wild Barley Diversity Collection (WBDC). Since its establishment, accessions in the WBDC have been screened for a variety of agronomic and morphological traits as well as diseases including stem rust, leaf rust, spot blotch, powdery mildew and other diseases and traits. Consistent high variation has been observed, including for resistance to these diseases, in micro-geographic and macro-geographic diversity in response to the diseases in general and considerable heterozygosity for the resistance genes in collection sites (Fetch et al., 2003). For example, genetic analysis of powdery mildew resistance within the WBDC was evaluated in one study. 316 accessions were screened with 40 isolates of *Blumeria graminis* f. sp. *hordei*, of which, three accessions, WBDC 053, WBDC 085, and WBDC

089 were resistant to 38 of the 40 isolates. GWAS identified 21 significant marker–trait associations corresponding to 15 QTL, seven of which had not previously been associated with powdery mildew resistance (Ames et al., 2015), highlighting the potential of wild barley to provide novel resistance genes absent or rare in cultivated germplasm. This collection was also screened for barley resistance against spot blotch caused by the fungus *Cochliobolus sativus*. All 318 WBDC accessions were screened, and remarkably 302 of 318 (95%) showed low infection responses. Association mapping identified 13 QTL for spot blotch resistance on chromosomes 1H, 2H, 3H, 5H, and 7H (Roy et al. 2010). Wild barley collections like the WBDC are a natural starting point for identifying novel FHB resistance absent in cultivated germplasm and the selected wild barley genotypes used in this study were selected from the WBDC collection.

1.6 Phenotyping approaches for evaluating FHB resistance

A major limitation in FHB resistance research is the availability of reliable and reproducible high-throughput phenotyping methods. Conventional phenotyping approaches including point- or spray-inoculation of spikes at anthesis and the subsequent scoring of symptom development over the following weeks is the standard method of field evaluation for resistance and is the most appropriate for assessing the resistance under actual field conditions (Buerstmayr et al., 2009; Mesterhazy, 2020; Boyles et al. 2024). However, field trials are laborious, season-limited, and are directly influenced by weather conditions. Inoculum density and escape from infection, resulting from differences in flowering time or plant height, between the various types of plants can mask real differences in resistance (Mesterhazy 2020). Although the greenhouse allows control over environmental conditions, it still involves plants being raised to anthesis prior to spike inoculation, and is a slow, space consuming process. Single-floret inoculation has proved to be less effective in discerning small, but genotypically significant, differences in resistance in the greenhouse using barley due to the fact that the rachis resistance level is generally high in barley preventing the spread of infection from spikelet to spikelet. These experiments remain relatively slow and space-consuming, and can become impractical when hundreds of genotypes, pathogen combinations or fungal isolates are to be evaluated. This is particularly unsuitable for screening the many genotypes required in the early stages of a breeding or germplasm-evaluation programme, where large numbers of accessions must often be evaluated before a smaller set of promising genotypes can be subjected to more detailed whole-plant and field testing. These constraints have led to the development of rapid, *in-vitro* assays, such as seed-germination assays, coleoptile inoculation and detached-organ assays that can simulate responses to whole plant infection, but require much less time, space and plant

material, and enable infection to be imposed under well standardized conditions (Browne & Cooke, 2004; Rafiei et al., 2025). Several of these approaches have shown significant associations with disease responses observed in adult plants, indicating their potential for rapid preliminary screening of large germplasm collections. More recently, Rafiei et al. (2025) directly compared detached-leaf, seedling, coleoptile, and conventional spike-infection assays for assessing wheat resistance and the virulence of different FHB-associated *Fusarium* species. The rapid assays were able to reproduce important patterns observed in spike infection, particularly differences in pathogen aggressiveness, with the seedling and coleoptile assays showing good agreement with disease responses observed in the conventional head assay. The detached-leaf assay also effectively differentiated *Fusarium* species according to virulence, although discrimination among wheat genotypes was less consistent. For genetically diverse resources such as wild barley collections, detached-leaf assay may prove especially useful approach. Screening hundreds of accessions through conventional head inoculations would require considerable greenhouse space, time, and resources, particularly when several *Fusarium* species and both single- and co-infection treatments are included.

1.7 The detached leaf assay as a rapid phenotyping tool

Detached leaf assay, one of the most popular methods used for pre-screening FHB resistance components, was originally developed and validated for wheat. In this assay, detached leaf segments are inoculated with a spore suspension of *Fusarium* or *Microdochium* species and grown under controlled conditions. The components of partial disease resistance such as incubation period, latent period and lesion length are measured under uniform environmental conditions, rather than in the field (Browne & Cooke, 2004). A comparative assessment of this approach with wheat, barley and oat cultivars found that the assay was able to discern partial resistance among all three species but the pattern of symptom expression varied, e.g., in wheat chlorosis was often more apparent at an earlier stage of symptom development whereas in barley chlorosis of lesions was not apparent until sporulation had begun (Browne & Cooke, 2005). Subsequent research has adapted and developed the detached leaf protocol specifically for wheat and for co-infection scenarios, and has also combined it with automated, image-based quantification of lesions to minimize subjectivity in lesion scoring (Perochon & Doohan, 2016). Recent comparative evaluations of detached leaf, coleoptile and seedling assays performed alongside conventional head-infection assay have confirmed that leaf-based assays can significantly reduce the time and resources required to separate FHB resistance and pathogen aggressiveness among *Fusarium* species. It can also offer a high throughput, rapid alternative to the

conventional field or greenhouse assays (Rafiei et al., 2025). Detached leaf assay is also highly suitable for screening large germplasm panels, including a wild barley diversity collection, or to compare single- and multi-species infection treatments side by side under identical conditions, which is more challenging to reliably produce in the field or with whole plants head assays.

1.8 Knowledge gaps and rationale

The literature reviewed above identifies three related knowledge gaps. First, although wild barley is recognized as an important source of resistance to several barley diseases, such as rust, powdery mildew, and spot blotch, the extent to which the Wild Barley Diversity Collection (WBDC) contains useful sources of resistance to FHB remains comparatively less characterized. Second, despite the fact that FHB is caused by a complex of species that frequently co-occur under field conditions, most resistance-screening studies in wheat and barley have focused on a single *Fusarium* species, particularly *F. graminearum*. Interactions among these species may influence disease development, mycotoxin production, and fungal colonization in non-additive ways. However, very few studies have investigated whether host resistance observed against a single species is sustained when plants are concurrently challenged by multiple FHB-associated *Fusarium* species. This knowledge gap is particularly evident for wild barley, where resistance responses under co-infection conditions remain poorly characterized. The third knowledge gap concerns the availability of rapid and reliable phenotyping approaches for screening large and genetically diverse germplasm collections. Conventional spike and field assays provide the most direct assessment of FHB resistance but are time, space, and resource-intensive. Rapid high-throughput phenotyping approaches such as detached-leaf assays provide an opportunity for preliminary screening under standardized conditions and have been evaluated primarily in wheat and, to a lesser extent, barley (Browne & Cooke, 2004, 2005; Rafiei et al., 2025). However, their application to diverse wild barley germplasm under single- and multi-species infection conditions, particularly in combination with objective digital image analysis of lesion development, remains limited. These gaps are directly addressed in this study by screening a subset of the WBDC for resistance to *F. graminearum* alone and by co-infection with *F. culmorum* and *F. avenaceum* using a rapid detached-leaf assay. Disease severity was assessed using both conventional visual scoring and digital image-based quantification of lesion development. The study therefore aimed to not only identify wild barley genotypes showing resistance or partial resistance, that may represent valuable material for future FHB resistance breeding, but also to assess the potential of the detached-leaf assay as a rapid and resource-efficient platform for large-scale, multi-species screening of diverse barley germplasm. Because screening all 318 WBDC accessions was not feasible

within the time frame of this project, a subset of 40 accessions was evaluated. The study combined a rapid detached leaf assay with two methods of disease assessment, conventional visual scoring and image-based quantification of lesion area, to address these gaps.

1.9 Aim and objectives

The aim of this study was to assess the response of wild barley genotypes to FHB pathogens under single-species and co-infection conditions using a detached leaf assay. The specific objectives were:

(1) to compare disease development in wild barley under single-species infection with *F. graminearum* and co-infection with *F. graminearum*, *F. culmorum* and *F. avenaceum*, and determine whether co-infection alters disease severity relative to single-species infection;

(2) to compare conventional visual disease scoring with image-based quantification of lesion area and evaluate their ability to discriminate between genotypes and infection treatments;

(3) to identify wild barley genotypes with resistance or partial resistance to single-species infection and co-infection as potential sources of resistance for future genetic studies and resistance breeding; and

(4) to evaluate the suitability of the detached leaf assay as a rapid phenotyping approach for screening large collections of barley germplasm for resistance to *Fusarium* infection.

2. Materials and Methods

2.1 Plant material

A subset of 40 wild barley (*Hordeum vulgare* subsp. *spontaneum*) accessions from the Wild Barley Diversity Collection (WBDC) were used in this study (Appendix 1). The WBDC consists of 318 genotyped accessions that have previously been evaluated for responses to several barley diseases (Steffenson et al., 2007; Spanner et al., 2026). Seed of the collection was provided by Prof. Brian Steffenson (Department of Plant Pathology, University of Minnesota, USA). The 40 accessions were selected at random from the collection. Country of origin was recorded for every accession from the WBDC data, so that the geographic coverage of the subset could be described. The selected accessions originated from 11 countries: Syria (12 accessions), Jordan (9), Iran (5), Afghanistan (4), Tajikistan (3), Palestine (2), and Lebanon, Pakistan, Egypt, Turkmenistan and Azerbaijan (one each). Thus, 24 accessions came from the core of the Fertile Crescent (Syria, Jordan, Lebanon and Palestine), and the remainder represented Iran, Central Asia, the Caucasus, South Asia and North Africa, broadly reflecting the geographic composition of the full collection. The accessions, their genebank (IG) numbers and countries of origin are listed in Appendix 1. Seed was multiplied in the greenhouse by the main supervisor prior to the experiments and is maintained in the cereal genotype collection at the Department of Forest Mycology and Plant Pathology, Swedish University of Agricultural Sciences (SLU), Uppsala.

2.2 Plant growth conditions

Seeds were sown in pots containing a standard peat-based potting soil in the greenhouse at SLU. Ten to twelve seeds were sown per pot to ensure sufficient germination, and after establishment the seedlings were thinned to five or six per pot to avoid competition. Pots with poor germination (one to three seedlings) were retained. Plants were first raised in a greenhouse at approximately 25 °C and then transferred to a phytotron at the Uppsala BioCenter (SLU), where they were grown at 20 °C under a 16 h light/8 h dark photoperiod. Plants were watered approximately twice a week, and no fertiliser was applied at any stage. Leaves for the detached leaf assay were harvested from plants approximately three weeks after sowing (Figure 1).



Figure 1. Barley genotypes cultivated in the greenhouse

2.3 Fungal isolates and inoculum preparation

Three FHB-associated *Fusarium* species were used: *F. graminearum, F. avenaceum* and *F. culmorum*. The isolates were obtained from the culture collection of the main supervisor at the Department of Forest Mycology and Plant Pathology, SLU. *F. graminearum* was strain PH1, originally isolated from wheat kernels in the USA, while the *F. culmorum* and *F. avenaceum* isolates were originally isolated from wheat in Sweden and provided by the Department of Ecology, SLU (Rafiei et al. 2025). Inoculum was produced following established protocols (Browne & Cooke 2004; Rafiei et al. 2025).

Three media were used because each serves a different purpose in producing *Fusarium* inoculum. Mung bean broth was used as the main liquid medium for production of macroconidia (Feng et al. 2018; Rafiei et al. 2025). Carboxymethyl cellulose (CMC) medium, a nutrient-poor liquid medium, was used because it induces abundant conidiation in submerged cultures of *Fusarium* species (Cappellini & Peterson 1965). Oatmeal agar was used as a solid medium for maintaining actively growing cultures and as a source of mycelial plugs for inoculating the liquid media. Mung bean broth was prepared by boiling 40 g of mung beans in 1 L of water, steeping for 40 min, filtering through cheesecloth and autoclaving the filtrate for 30 min. CMC medium was prepared by dissolving 15 g of carboxymethyl cellulose sodium salt in hot water with continuous stirring and adding NH_4NO_3 (1 g L^{-1}), KH_2PO_4 (1 g L^{-1}), $MgSO_4 \cdot 7H_2O$ (0.5 g L^{-1}) and yeast extract (1 g L^{-1}), after which the volume was adjusted to 1 L and the medium was autoclaved. Oatmeal agar was prepared from 10 g of oatmeal and 12 g of malt extract agar per litre and autoclaved for 30 min. After sterilisation, kanamycin (50 µg mL^{-1}) was added to all media to suppress bacterial contamination. Oatmeal agar was poured into Petri dishes, and the liquid media were dispensed into Erlenmeyer flasks (50 mL per flask). Mycelial plugs of each species were

transferred to the plates and flasks, and cultures were incubated at 25 °C in darkness; liquid cultures were incubated on a rotary shaker at 150 rpm for 14–20 days until harvest (Figure 2).

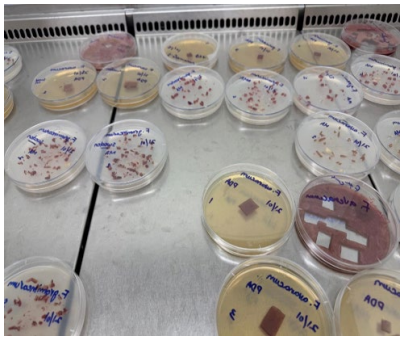


Figure 2. Preparing fungal mycelia and inoculum for screening barley genotypes

2.3.1 Spore harvesting

Conidia were harvested after 14–20 days of incubation. Liquid cultures were filtered directly through sterile Miracloth (Merck Millipore, Darmstadt, Germany) to remove mycelial fragments. For cultures on agar plates, the plates were first flooded with sterile distilled water and the colony surface was gently scraped with a sterile spreader to release the conidia, after which the suspension was filtered through Miracloth in the same way (Rafiei et al., 2025).

2.3.2 Spore counting

Spore concentration was determined by loading a 10 µL aliquot of well-mixed conidial suspension onto a hemocytometer and examining it under a light microscope. Spores were counted in five selected squares (four corner squares and the central square) to ensure representative estimation of density. The mean number of spores per square was converted to spores per millilitre as: spores mL^{-1} = mean count per square × dilution factor / volume of one square (mL). For a large hemocytometer square (1 mm^2 × 0.1 mm depth = 0.1 µL), this equals the mean count × 10^4 × dilution factor. Following quantification, spore suspensions were adjusted with sterile distilled water to a final concentration of 1 × 10^6 spores/mL, which was used for all inoculation treatments (Browne & Cooke 2005).

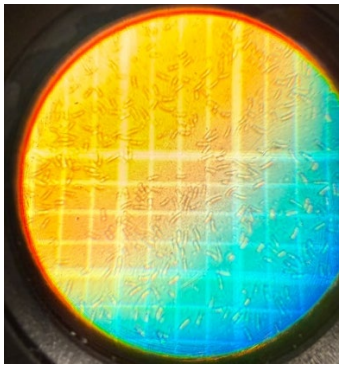


Figure 3. Counting and adjusting the spores of Fusarium *species on a hemocytometer*

2.4 Detached leaf assay

A detached leaf assay was used to evaluate the response of the wild barley accessions to FHB pathogens under controlled conditions, following Browne & Cooke (2004) with the modifications of Perochon & Doohan (2016) and Rafiei et al. (2025). This system allows standardized infection and phenotyping under uniform environmental conditions.

2.4.1 Experimental design, biological and technical replication

Three treatments were applied to each accession: (i) a mock-inoculated control (sterile distilled water), (ii) single-species infection with *F. graminearum* (Fg), and (iii) co-infection with *F. graminearum*, *F. avenaceum* and *F. culmorum* (Mix). Three biological replicates were prepared for each accession and treatment. Each biological replicate consisted of one Petri dish containing four detached leaves, which served as technical replicates. The full design therefore comprised 40 accessions × 3 treatments × 3 biological replicates.

2.4.2 Leaf preparation and placement

Leaves were harvested from approximately three-week-old plants across genotypes, selecting fully expanded leaves from similar positions to reduce variation due to plant development. Initially, six detached leaves per Petri dish were used; however, this number was later reduced to four leaves per plate to improve handling and ensure more consistent infection and phenotyping. Detached leaves were placed horizontally onto Petri dishes containing solidified agar medium, consisting of 15 g Bacto-agar in 500 mL distilled water, followed by autoclaving. After sterilization and cooling, benzimidazole (30 mg L^{-1}) was added to delay leaf senescence, and kanamycin (50 µg mL^{-1}) was included to reduce bacterial contamination. Approximately 50 mL of medium was poured per plate and allowed to solidify before leaf placement. Sections of thick agar were placed at both ends of each leaf to secure them in position and prevent curling

(Figure 4) or displacement during incubation (Browne & Cooke, 2005; Perochon & Doohan, 2016). Prior to inoculation, leaves were gently wounded using a sterile pipette tip to facilitate fungal penetration and ensure infection. For the single-species treatment, the *F. graminearum* conidial suspension was adjusted to 1×10^6 spores mL^{-1}. For the co-infection treatment, suspensions of the three species (*F. graminearum*, *F. avenaceum* and *F. culmorum*), each adjusted to 1×10^6 spores mL^{-1}, were mixed in equal volumes, giving a total concentration of 1×10^6 spores mL^{-1} with approximately 3.3×10^5 spores mL^{-1} of each species. A volume of 30 µL of inoculum was applied onto the central part of each leaf using a micropipette. Mock controls received sterile distilled water in the same volume. After inoculation, plates were sealed and transferred to controlled phytotron conditions for incubation at 20°C under a 16 h light/8 h dark photoperiod at 80% humidity. Disease development was monitored under uniform environmental conditions across all treatments (Rafiei et al., 2025).



Figure 4. Detached leaf assay and inoculation of barley leaves with Fusarium *species*

2.5 Disease assessment and digital image analysis

Disease development was assessed using both visual scoring and digital image analysis to quantify lesion progression on detached barley leaves. Preliminary imaging trials were conducted at different time points (3, 5, 6, and 7 days post inoculation, DPI) after inoculation to determine the optimal stage for phenotyping. Initial assessments at 3 DPI indicated that lesion development was insufficient for reliable discrimination between resistant and susceptible genotypes. At 6–7 DPI, lesions had expanded so far that symptom expression became saturated, which reduced the ability to distinguish intermediate levels of resistance. Prolonged incubation is also less suitable because detached leaves lack systemic defence responses and begin to senesce. Based on iterative testing across different time points, 5 DPI was selected as the optimal time point for digital imaging and disease assessment, as it provided the best balance between lesion visibility and discrimination among genotypes.



Figure 5. Incubation of inoculated detached leaves of different barley genotypes in the growth chambers at different time points

2.5.1 Digital imaging

Digital imaging was performed at 5 DPI to monitor lesion development. Images were captured using a fixed camera setup under standardized conditions. The camera was operated in manual mode with automatic focus enabled. Imaging settings were standardized as follows: image quality RAW + JPEG, ISO 200, aperture f/10, shutter speed 1/30 s, and focal length 18 mm. The camera was positioned at a fixed distance of 35 cm above the imaging platform to ensure consistency across all samples.



Figure 6. Digital imaging of lesion size of inoculated leaves for each treatment and genotype

2.5.2 Disease scoring and visual assessment

Initial phenotyping was performed using a visual scoring system based on lesion development. By visually analyzing various photographs, a comparative disease scale ranging from 0 to 8 was developed, where scores represented increasing levels of lesion size and severity. Each detached leaf was visually compared

against this reference scale and assigned a corresponding score. Visual scoring provided a rapid assessment that was analysed in parallel with, and compared against, the image-based measurements. For each biological replicate, the disease index was calculated as the mean score of the leaves in the Petri dish.

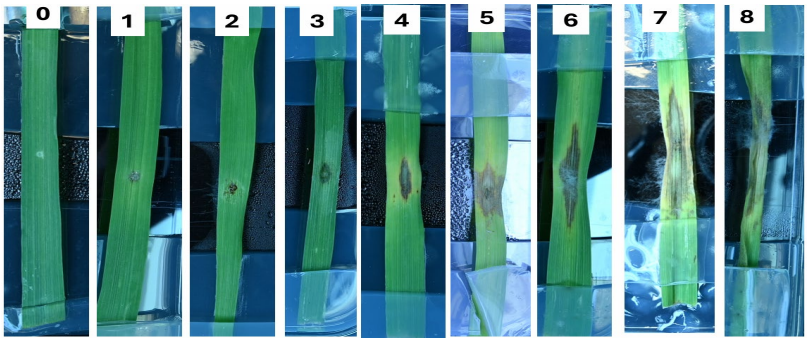


Figure 7. Disease scoring scale from 0 to 8 corresponding to the level of severity and lesion size caused by Fusarium *infection that was used as a reference for visual disease assessment*

2.5.3 Image-based lesion quantification

For quantitative analysis, lesion areas were measured using ImageJ software (Schneider et al. 2012). To minimize observer bias, digital image analysis was used as the primary method for final disease quantification. Each image was first calibrated using a reference scale included in the image, converting pixel measurements into millimetres in ImageJ software. After setting the spatial scale, images were processed in ImageJ for lesion quantification. Initially, lesion area estimation was attempted using colour thresholding; however, due to variability in lesion coloration and background heterogeneity, this approach was not sufficiently consistent across samples. Therefore, lesion areas were manually delineated using the freehand selection tool for each image. Only the necrotic lesion was measured, the yellow, chlorotic halo surrounding some lesions was excluded from the lesion area. For each biological replicate, the ImageJ disease index was calculated as the mean lesion area (mm^2) of the four leaves in the dish. The final workflow in ImageJ was as follows:
Image > Drag and Drop > Set Scale > Pixels into mm > Set Global > Freehand selection > Ctrl + M

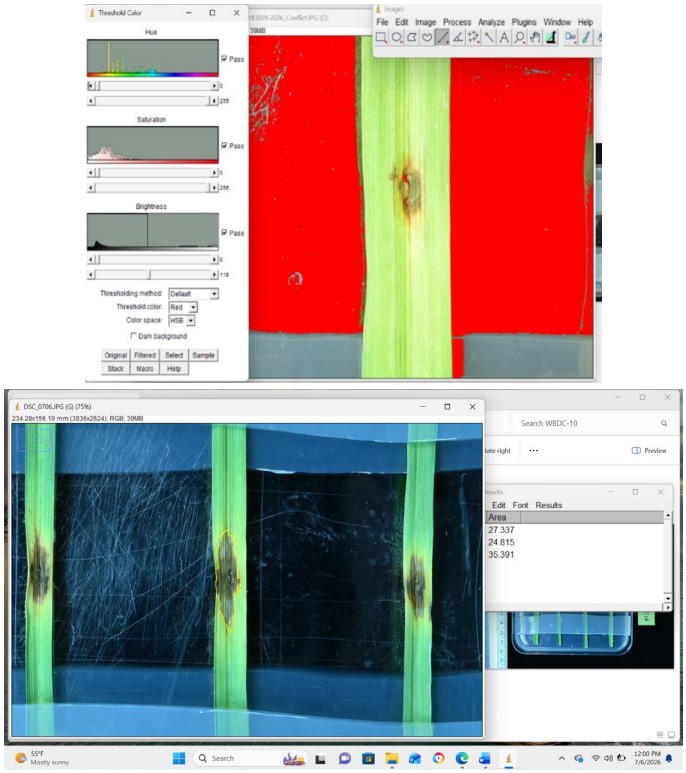


Figure 8. Measurement of lesion area in ImageJ: calibration of the image scale (left) and manual delineation of the necrotic lesion, excluding the chlorotic halo (right)

2.5.4 Data processing and statistical analysis

Lesion area measurements and visual disease scores were statistically analyzed to compare disease responses among genotypes and treatments. All statistical analyses were performed in R (R Core Team, 2024). Lesion area data were used as the primary quantitative response variable, while visual scores were used for comparative and validation purposes. For each scoring method, the disease index of each biological replicate (Petri dish) was analysed with a two-way analysis of variance (ANOVA) with genotype, treatment and their interaction as fixed effects. The ImageJ disease index (mean lesion area, mm^2) was strongly right-skewed (skewness = 3.78) and its variance increased with disease severity; it was therefore transformed as $\log_2(DI + 1)$ before analysis, which reduced the skewness to 0.11. When significant effects were detected, treatments were compared using estimated marginal means with Tukey's honestly significant difference (HSD) adjustment, and *F. graminearum* and Mix infection were compared within each genotype in the same way. Genotypes were ranked by their mean disease index averaged across the three treatments. To describe how co-infection changed disease relative to single-species infection, a co-infection effect was calculated for each genotype as the difference in mean lesion area (mm^2, untransformed) between the Mix and *F. graminearum* treatments.

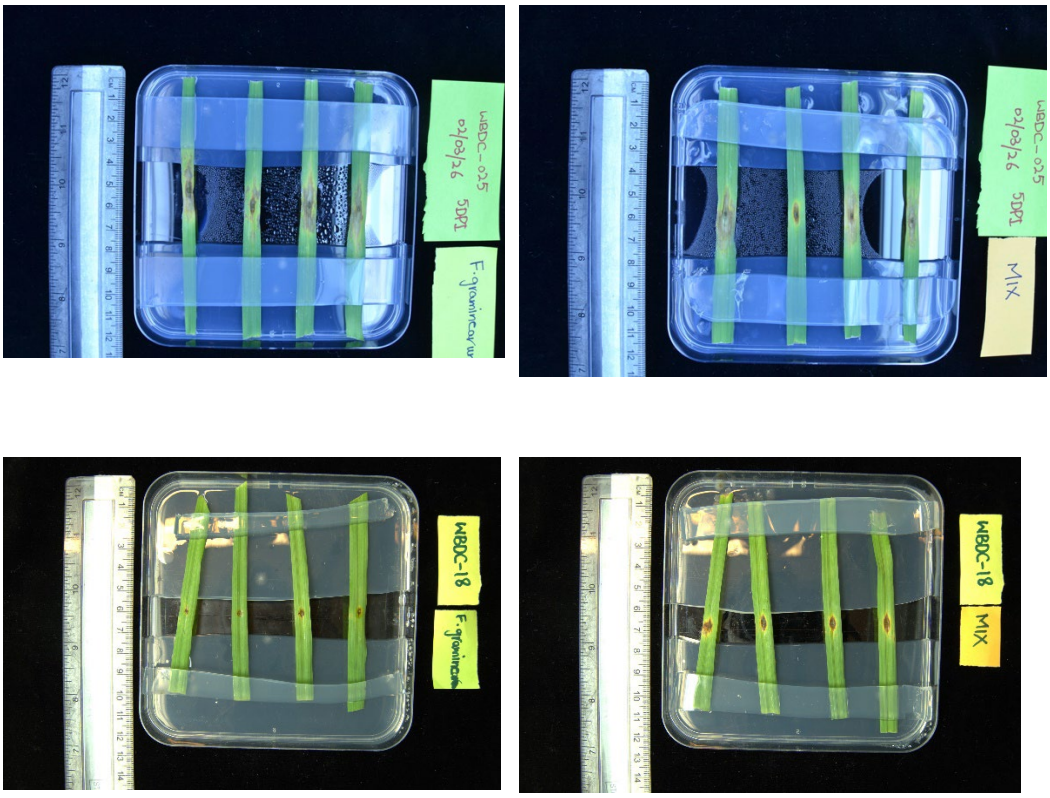


Figure 9. Representative lesion development in the susceptible genotype WBDC-10 (upper panel) and the less susceptible genotype WBDC-18 (lower panel) under single and co-infection treatments

2.5.5 Repeat trial and selection of genotypes for molecular analysis

A subset of genotypes representing the extremes of the susceptibility range in the initial screen was selected for repeat cultivation and inoculation to assess the reproducibility of the phenotypic results and obtain additional tissue for molecular analysis. Molecular analysis comprised FG16N PCR assays and *Tri13* gene-specific PCR assays to distinguish DON- and NIV-associated trichothecene

genotypes based on polymorphisms within the *Tri13* gene (Chandler et al. 2003). In the repeat trial, WBDC-060, WBDC-034 and WBDC-012 (among the least susceptible) and WBDC-110, WBDC-164 and WBDC-159 (among the most susceptible) were regrown and re-inoculated under the same single-species (*F. graminearum*) and co-infection (Mix) conditions described in Sections 2.3–2.4. Only WBDC-060 and WBDC-159 produced enough tissue suitable for downstream molecular analysis. Genomic DNA extracted from the repeat-cultivation samples of WBDC-060 and WBDC-159 was used for the FG16N, DON, and NIV PCR assays described in Sections 2.6–2.7. Molecular analysis was consequently restricted to these two genotypes, representing the lower and upper ends of the susceptibility range, respectively.

2.6 DNA extraction

Genomic DNA was extracted from infected leaf tissue using a modified cetyltrimethylammonium bromide (CTAB) method (Inglis et al. 2018) as described below. Following disease assessment, lesion tissue was excised from infected leaves, freeze-dried, and stored at −20 °C prior to extraction. The CTAB extraction buffer (3%) was prepared using Tris-HCl, NaCl, EDTA, and CTAB in Milli-Q water. Approximately 600 µL of CTAB buffer was added to each sample, followed by thorough homogenization with a sterile micro-pestle. Samples were incubated at 65 °C for 30–60 minutes to facilitate cell lysis and release of nucleic acids, with occasional shaking. Samples were then centrifuged at 10,000 rpm for 10 minutes, and the supernatant was transferred to a new 1.5 mL microcentrifuge tube. An equal volume of chloroform:isoamyl alcohol (24:1) was added, and samples were mixed by inversion and centrifuged at 10,000–13,000 rpm for 10–15 minutes. The supernatant was carefully transferred to a new 1.5 mL microcentrifuge tube. A second chloroform extraction was performed to improve purity, and the aqueous phase was again recovered after centrifugation. DNA was precipitated by adding an equal volume of cold isopropanol and incubating at −20 °C for 20 minutes. Samples were then centrifuged at 13,000 rpm for 15–20 minutes to pellet the DNA. The supernatant was discarded, and the pellet was washed with 200 µL of 70% ethanol followed by centrifugation at 13,000 rpm for 5 minutes. After removal of ethanol, pellets were air-dried and resuspended in 50 µL TE buffer. DNA quality and concentration were assessed using NanoDrop spectrophotometer.

2.7 PCR reagents and amplification conditions

The presence of *F. graminearum* in single-species and co-infected leaf tissue was tested by conventional polymerase chain reaction (PCR) using the species-specific primer pair Fg16N, originally developed by Nicholson et al. (1998). In addition,

trichothecene chemotypes were determined using Tri13 gene-specific primers capable of distinguishing deoxynivalenol (DON)- and nivalenol (NIV)-producing isolates based on polymorphisms within the *Tri13* gene (Chandler et al., 2003). Species identification was performed using the Fg16N primer pair (Fg16NF: 5′-ACAGATGACAAGATTCAGGCACA-3′ and Fg16NR: 5′-TTCTTTGACATCTGTTCAACCCA-3′), which amplifies an approximately 280 bp fragment specific to *F. graminearum*. These primers did not amplify DNA of *F. culmorum* or the other *Fusarium* species tested by Nicholson et al. (1998), so a positive result indicates *F. graminearum* specifically. Each PCR reaction contained approximately 50 ng of template DNA, 1× DreamTaq Green buffer, 200 µM of each dNTP, 0.2 µM of each FG16N primer (forward and reverse), and 0.5 U DreamTaq DNA polymerase. Nuclease-free water was added to a final reaction volume of 20 µL. PCR was performed using the FG16N primers described by Nicholson et al. (1998), with the thermal cycling programme optimized for this study on an Applied Biosystems VeritiPro thermal cycler as follows: an initial denaturation at 95 °C for 1.5 min, followed by 35 cycles of denaturation at 94 °C for 30 s, annealing at 64 °C for 45 s, and extension at 72 °C for 45 s, with a final extension step at 72 °C for 5 min and a final hold at 12 °C. PCR products were verified by agarose gel electrophoresis.

2.7.1 Detection of trichothecene biosynthesis genes (DON and NIV primers)

In addition to the species-confirmation FG16N assay, PCR assays using primer sets specific to the trichothecene biosynthesis gene were used to screen genes associated with deoxynivalenol (DON) and nivalenol (NIV) chemotypes. Trichothecene chemotypes were determined using Tri13 gene-specific primer sets. The DON-specific primer pair Tri13DONF: 5′-CATCATGAGACTTGTKCRAGTTTGGG-3′ and Tri13DONR: 5′-GCTAGATCGATTGTTGCATTGAG-3′ amplified an expected fragment of approximately 282 bp, whereas the NIV-specific primer pair, Tri13NIVF: 5′-CCAAATCCGAAAACCGCAG-3′ and Tri13NIVR: 5′-TGAAAGCTCCAATGTCGTG-3′ generated an approximately 312 bp fragment in NIV-producing isolates. These primers were developed to determine the chemotype of *F. graminearum*, *F. culmorum* and *F. cerealis* (Chandler et al., 2003), so in the co-infection treatment they can amplify Tri13 from *F. culmorum* as well as from *F. graminearum*. These assays were performed on genomic DNA extracted from wild barley genotypes WBDC-060 (least susceptible genotype) and WBDC-159 (highly susceptible genotype) under single-species (*F. graminearum* only) and co-infection (mixed-species) treatments.Each PCR reaction contained 4 µL of 10× DreamTaq Green buffer, 2 µL of dNTPs, 0.5 µL of each primer (forward and reverse), and 0.2 µL of DreamTaq DNA polymerase,

made up to a final master-mix volume of 19 µL per reaction with nuclease-free water; 1 µL of template DNA was added per reaction to give a final reaction volume of 20 µL, consistent with the FG16N assay format described above. Master mix was prepared in batches of 25 reactions per primer set. DON and NIV assays were amplified using the same thermal cycling programme described for the FG16N assay (Section 2.7).

2.7.2 Agarose gel electrophoresis and PCR product visualization

PCR products were separated by electrophoresis on a 1 % agarose gel prepared in sodium borate (SB) buffer. Electrophoresis was performed alongside a 1kb DNA ladder, and amplified fragments were visualized under UV using Gel Documentation System to confirm amplicon presence.

3. Results

3.1 Phenotypic analysis based on visual scoring

A two-way analysis of variance (ANOVA) was conducted to evaluate the effects of genotype, treatment, and their interaction on disease index. The results revealed that treatment had a highly significant effect on disease development ($F_{2,252}$ = 528.59, $p < 0.001$). Similarly, genotype significantly influenced disease index ($F_{41,252} = 5.79$, $p < 0.001$). Importantly, a significant genotype × treatment interaction was observed ($F_{82,252} = 4.53$, $p < 0.001$), indicating that genotypes responded differently to the applied treatments (Table 1). Post-hoc comparisons using Tukey's HSD test showed that all treatments differed significantly from each other. Disease severity was lowest under control conditions and increased significantly under *F. graminearum* inoculation, with the highest disease index observed under mixed infection ($p < 0.001$ for all comparisons) (Table 2). Substantial variation in disease response was observed among genotypes. Genotypes such as WBDC-110, WBDC-164, and WBDC-010 exhibited the highest mean disease indices, indicating high susceptibility, while genotypes such as WBDC-060, WBDC-120, and WBDC-034 showed the lowest mean disease indices, suggesting partial resistance (Table 3). The significant interaction between genotype and treatment further demonstrated that the relative susceptibility of genotypes varied depending on the type of infection, with some genotypes showing increased sensitivity specifically under mixed infection conditions rather than a uniform escalation of disease across all genotypes (Figure 10). This pattern was examined in more detail using the continuous ImageJ-based measurements (Section 3.2), which allowed the shape of individual genotype responses across treatments to be visualised directly.

Table 1. Two-way ANOVA for Disease Index (visual scoring)

Source	df	Sum Sq	Mean Sq	F value	p-value
Genotype	41	195.41	4.77	5.79	< 0.001 ***
Treatment	2	869.62	434.81	528.59	< 0.001 ***
Genotype × Treatment	82	305.25	3.72	4.53	< 0.001 ***
Residuals	252	207.29	0.82		

Table 2. Pairwise comparisons of treatments based on estimated marginal means using Tukey's post-hoc test (visual scoring)

Comparison	Estimate	p-value
Control vs *F. graminearum*	-2.63	< 0.001
Control vs Mix infection	-3.59	< 0.001
F. graminearum vs Mix	-0.96	< 0.001

Table 3. Most and least susceptible genotypes (visual scoring)

Most susceptible genotypes

Rank	Genotype	Mean Disease Index
1	WBDC-110	3.78
2	WBDC-164	3.67
3	WBDC-10	3.28
4	WBDC-159	3.06
5	WBDC-254	2.86
6	WBDC-109	2.83
7	WBDC-225	2.83

Least susceptible genotypes

1	WBDC-060	0.50
2	WBDC-120	0.86
3	WBDC-034	0.97
4	WBDC-123	1.11
5	WBDC-221	1.22
6	WBDC-005	1.39
7	WBDC-012	1.53

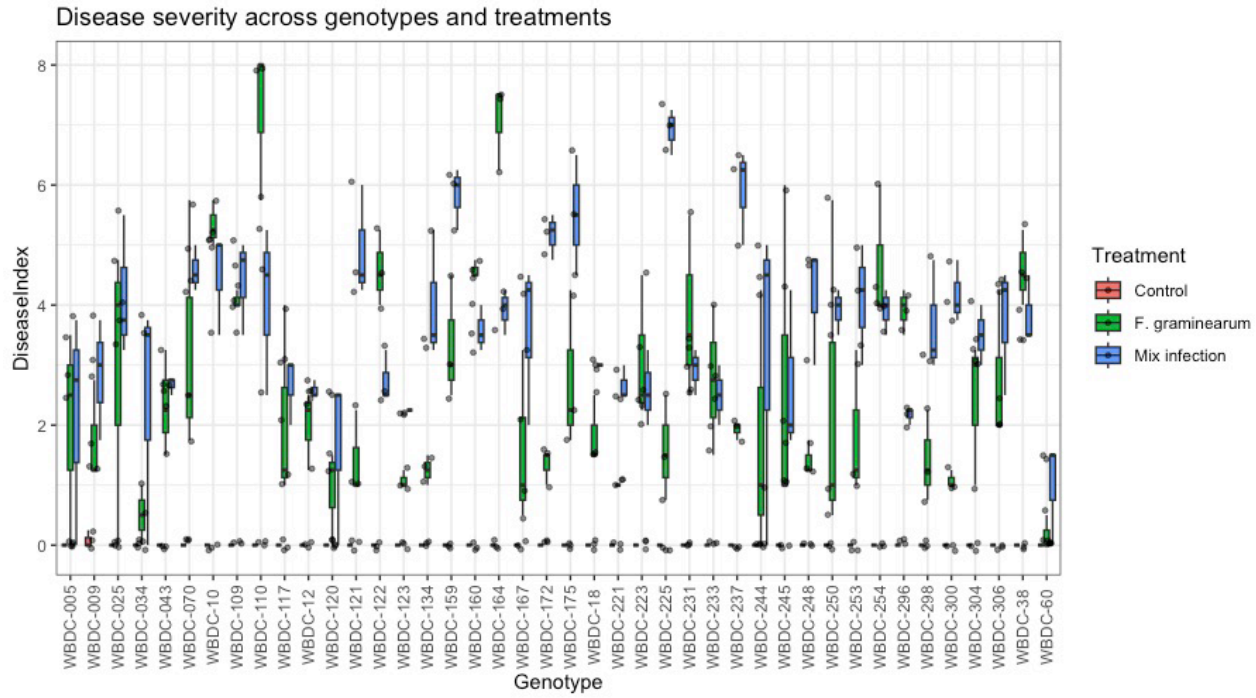


Figure 10. Disease index (mean visual score per Petri dish, 0–8 scale) of individual genotypes under control, single infection, and mixed infection conditions

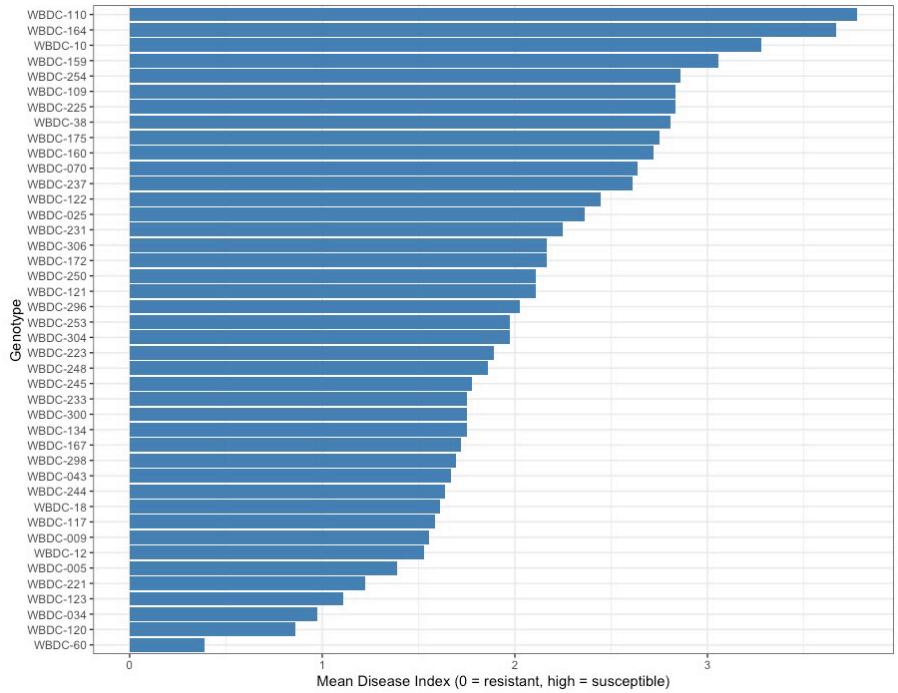


Figure 11. Overall susceptibility of genotypes based on mean disease index averaged across all treatments (visual scoring). Higher values indicate greater susceptibility (0 = no symptoms, 8 = most severe)

3.2 Phenotypic analysis

Leaf lesion area was additionally quantified for the 40 genotypes using ImageJ, giving a continuous disease index for each genotype under each treatment, which was analysed on the $\log_2(DI + 1)$ scale (Section 2.5.4; Table 4). The results revealed that treatment had a highly significant effect on disease development ($F_{2,240} = 670.24$, $p < 0.001$) and accounted for the majority of explained variance in the model (65.8% of total sum of squares), confirming that infection status was the dominant driver of disease severity. Genotype also significantly influenced disease index ($F_{39,240} = 5.03$, $p < 0.001$; 9.6% of variance), and, importantly, a significant genotype × treatment interaction was observed ($F_{78,240} = 3.35$, $p < 0.001$; 12.8% of variance) — a larger share of variance than genotype alone — indicating that genotypes responded differently to the applied treatments rather than simply shifting up or down together. Post-hoc comparisons using Tukey's HSD test showed that all treatments differed significantly from each other. Disease severity was lowest under control conditions and increased significantly under *F. graminearum* inoculation, with the highest disease index observed under mixed infection ($p < 0.001$ for all comparisons) (Table 5). Substantial variation in disease response was observed among genotypes. Genotypes such as WBDC-245, WBDC-164, and WBDC-110 exhibited the highest mean disease indices, indicating high susceptibility, while genotypes such as WBDC-060, WBDC-120, and WBDC-034 showed the lowest mean disease indices, suggesting partial resistance (Table 6, Figure 12). Within-genotype comparisons of *F. graminearum* versus Mix infection, annotated directly in Figure 13, showed a statistically significant difference for 21 of the 40 genotypes tested (Tukey HSD, $p < 0.05$). This ranged from highly significant differences in genotypes such as WBDC-172, WBDC-164, and WBDC-122 ($p < 0.001$) to more marginal differences in genotypes such as WBDC-117 and WBDC-175 ($p < 0.05$); the remaining 19 genotypes did not differ significantly between the two infection treatments, despite the highly significant interaction term overall, indicating that the genotype × treatment interaction was driven by a substantial subset of genotypes rather than a uniform effect across the panel. The direction of the co-infection effect also differed among genotypes (Figure 13). For most genotypes, disease index was higher under Mix infection than under *F. graminearum* alone. However, WBDC-110 and WBDC-164, the two most severely affected genotypes under *F. graminearum* alone, showed a marked reduction in disease index under Mix infection, whereas WBDC-237 and WBDC-175 showed the reverse, with disease index highest under Mix infection and comparatively low under *F. graminearum* alone. To quantify this, the co-infection effect (the difference in mean lesion area between Mix infection and *F. graminearum* alone) was calculated for each genotype (Table 7, Figure 14). Genotypes with a large positive difference showed disease potentiation under co-infection, most notably WBDC-237 and WBDC-

175; genotypes with a large negative difference showed disease suppression under co-infection, most strongly WBDC-110 and WBDC-164. Taken together, the visual scoring and ImageJ-based analyses (Sections *3.*1 and *3.2*) identified a consistent core set of genotypes at both extremes of the susceptibility range: WBDC-110 and WBDC-164 were among the most susceptible genotypes under both scoring approaches, while WBDC-060 and WBDC-034 were among the least susceptible under both. WBDC-060, WBDC-034 and WBDC-120 were the three least susceptible genotypes with both methods (Tables 3 and 6), indicating that the ranking at the extremes of the range did not depend on the scoring method used.

Table 4. Two-way ANOVA for Disease Index (ImageJ-based quantification, log2-transformed)

Source	df	Sum Sq	Mean Sq	F value	p-value
Genotype	39	180.59	4.63	5.03	< 0.001 ***
Treatment	2	1233.02	616.51	670.24	< 0.001 ***
Genotype × Treatment	78	240.00	3.08	3.35	< 0.001 ***
Residuals	240	220.76	0.92		

Table 5. Pairwise comparisons of treatments based on estimated marginal means using Tukey's post-hoc test (log2 scale)

Comparison	Estimate	p-value
Control vs *F. graminearum*	−3.55	< 0.001
Control vs Mix infection	−4.22	< 0.001
F. graminearum vs Mix	−0.67	< 0.001

Table 6. Most and least susceptible genotypes (ImageJ-based quantification; mean log2(DI + 1) across treatments)

Most susceptible genotypes		
Rank	**Genotype**	**Mean $\log_2$(DI + 1)**
1	WBDC-245	4.02
2	WBDC-164	3.99
3	WBDC-110	3.93
4	WBDC-159	3.84
5	WBDC-254	3.71
6	WBDC-109	3.59
7	WBDC-233	3.50
Least susceptible genotypes		
1	WBDC-060	1.33
2	WBDC-034	1.49
3	WBDC-120	1.67
4	WBDC-005	1.92
5	WBDC-018	2.01
6	WBDC-009	2.03
7	WBDC-012	2.04

Table 7. Co-infection effect for selected genotypes: mean lesion area (mm², untransformed) under each treatment and the difference between Mix infection and F. graminearum *alone (ImageJ quantification)*

Genotype	**Control**	***F. graminearum***	**Mix infection**	**Difference (Mix − Fg)**
WBDC-237	0.06	5.19	99.91	+94.72
WBDC-175	0.00	18.85	74.46	+55.61

WBDC-110	0.00	192.92	23.95	−168.97
WBDC-164	0.00	138.43	28.29	−110.14

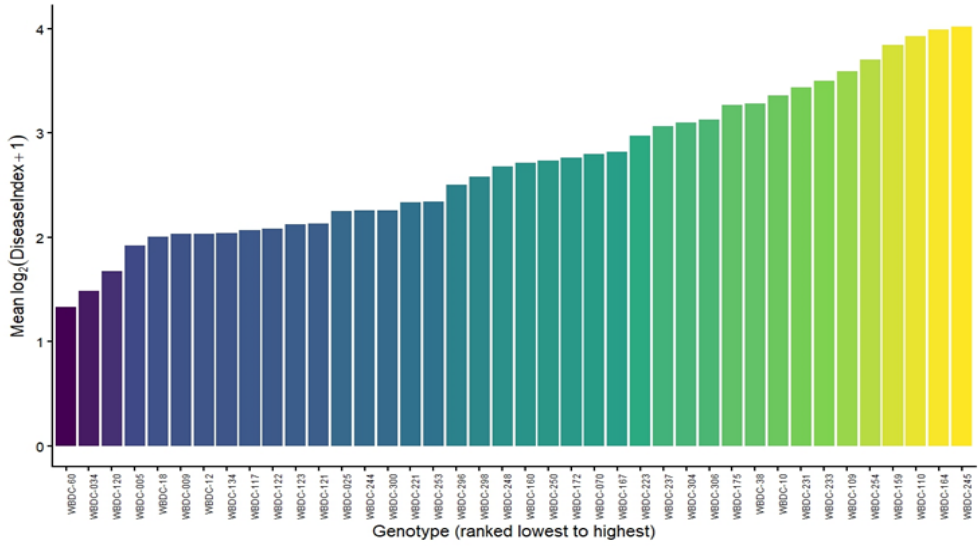


Figure 12. Overall susceptibility of genotypes based on mean log2(DiseaseIndex + 1) averaged across all treatments (ImageJ). Higher values indicate greater susceptibility

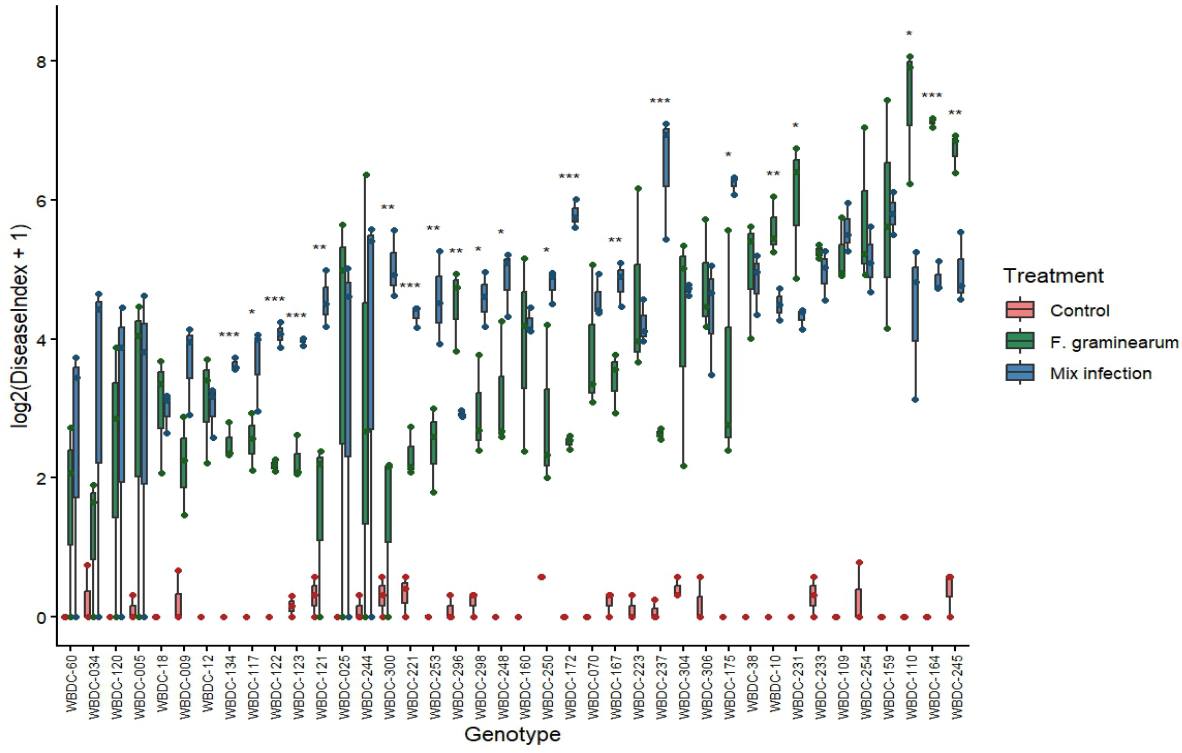


Figure 13. Mean log2(DiseaseIndex + 1) by genotype and treatment, with asterisks denoting Tukey-adjusted significance

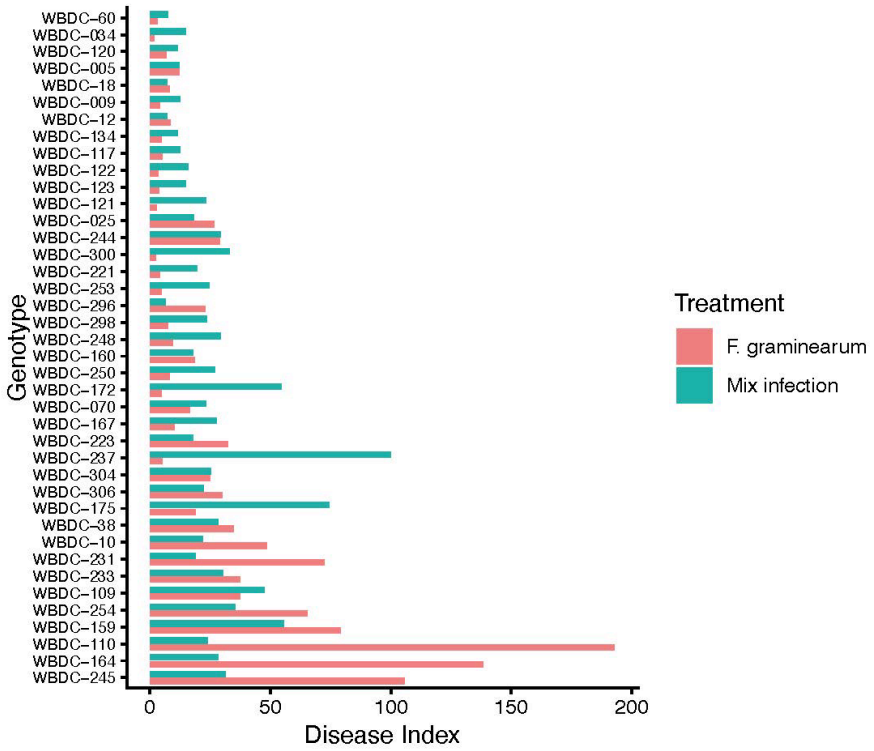


Figure 14. Mean ImageJ disease index (lesion area) under single-species inoculation with F. graminearum *and mixed-species inoculation (Mix) for each genotype; the difference between the two treatments is the co-infection effect (Section 2.5.4; Table 7)*

3.3 PCR detection of *F. graminearum* and Tri13 sequences

Molecular analyses were carried out on WBDC-060 and WBDC-159 from the repeat trial (Section 2.5.5). Amplification of the expected FG16N product was obtained in DNA extracted from WBDC-060 infected with *F. graminearum* and from WBDC-159 infected with *F. graminearum*. All corresponding co-infection replicates (WBDC-060, WBDC-159) were negative for this assay (Figure 15).

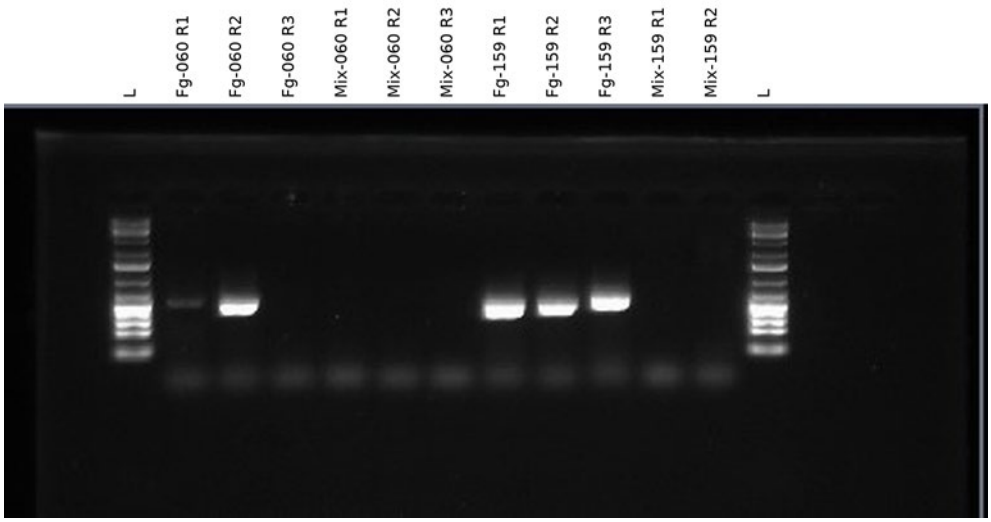


Figure 15. PCR detection of Fusarium graminearum *DNA (FG16N assay) in WBDC-060 and WBDC-159 under the* F. graminearum *(Fg) and co-infection (Mix) treatments. Lane labels give the treatment, genotype and biological replicate (R); L = 1 kb DNA ladder*

PCR using DON- and NIV-specific primers was performed on the same set of DNA samples. Using the DON-specific primers, amplification was obtained exclusively in the co-infection (Mix) samples of both genotypes WBDC-060 and WBDC-159 (four of four replicates positive), while *F. graminearum*-only samples were negative, with the exception of a single faint, trace-level amplification product in one WBDC-060 Fg-only replicate. No amplification was obtained with the NIV-specific primers in any sample, under either infection treatment or genotype (Figure 16).

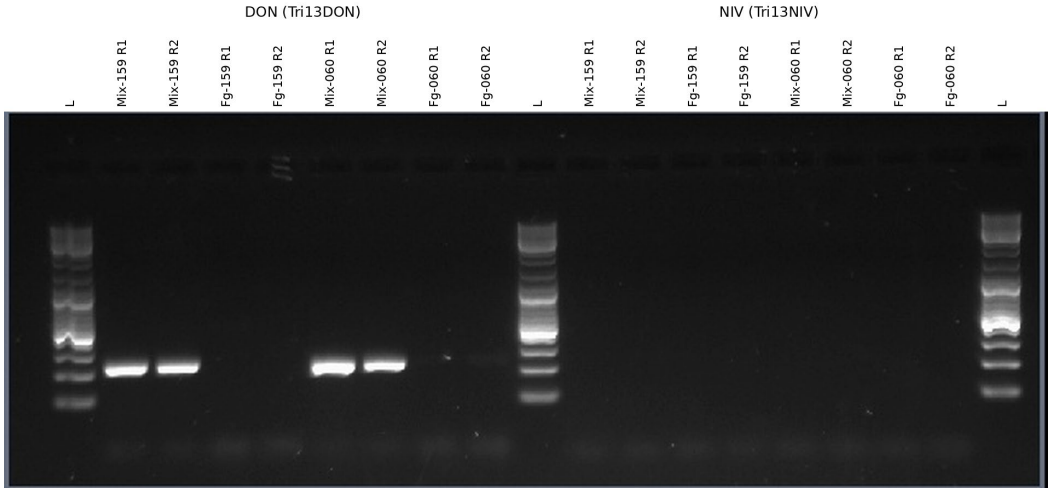


Figure 16. PCR screening for DON-associated (left) and NIV-associated (right) Tri13 sequences in WBDC-060 and WBDC-159 under the F. graminearum *(Fg) and co-infection (Mix) treatments. Lane labels give the treatment, genotype and biological replicate (R); L = 1 kb DNA ladder*

4. Discussion

Significant variation in FHB susceptibility and resistance was observed in wild barley genotypes screened in this study, in agreement with the polygenic and quantitative nature of FHB resistance reported in cultivated barley (Massman et al. 2011) and endorsing earlier surveys of *Hordeum vulgare* subsp. *spontaneum* showing that wild barley carries diverse, largely unexplored sources of disease resistance (Fetch et al., 2003). Genotypes such as WBDC-060 and WBDC-034 consistently ranked among the least susceptible genotypes with both the visual scoring and the ImageJ-based analyses, making them promising candidates for further validation under field or whole-plant conditions, and in-depth molecular characterisation. In addition, these genotypes together with most susceptible ones, such as WBDC-110 and WBDC-164, could potentially form a useful contrasting panel for future mechanistic or mapping studies (Steffenson et al., 2007). This pattern is broadly consistent with mapping studies in wild barley carried out for other fungal diseases. Roy et al. (2010) identified multiple quantitative trait loci (QTLs) for spot blotch resistance segregating widely across wild barley accessions, and Ames et al. (2015) similarly reported significant variation in powdery mildew resistance across the WBDC. The consistent placement of WBDC-060 among the least susceptible genotypes, and of WBDC-110, WBDC-164 and WBDC-159 among the most susceptible, with both scoring methods suggests that these represent genuine differences in susceptibility rather than experimental noise. These phenotypes should nevertheless be confirmed in independent repeat experiments before the genotypes are used for mapping, in line with Steiner et al. (2009), who emphasised phenotypic reproducibility as a prerequisite for reliable QTL mapping. Additionally, the partially resistant genotypes identified originate from different countries: WBDC-060 from Egypt, WBDC-034 from Palestine and WBDC-120 from Tajikistan (Appendix 1). Although the random sample was too small to be tested for geographic patterns, this suggests that useful variation may not be confined to one region.

A central aim of this study was to compare a conventional, scorer-dependent visual disease scale against an objective, image-based quantification method. Both approaches identified the same overall pattern: a highly significant effect of treatment, considerable genotypic variation, and a significant genotype-by-treatment interaction, and both approaches highlighted a broadly similar set of resistant and susceptible genotypes. At the same time, the ImageJ-based method offers a continuous measure of lesion area that depends less on the scorer's judgement and is less prone to the compression at the extremes of an ordinal scale (for example, distinguishing a very small lesion from no lesion at all), and it allowed the co-infection effect to be expressed in absolute lesion area (mm^2), which the ordinal visual scale cannot provide. Taken together, the two methods

are best viewed as complementary rather than interchangeable: visual scoring remains fast and requires no specialised equipment, making it attractive for large-scale first-pass screening, while image-based quantification is better suited to more detailed characterisation of a shortlisted set of genotypes. This agreement between visual and image-based scoring is in line with the findings of Perochon & Doohan (2016), who validated an image-analysis pipeline for detached-leaf FHB assays in wheat, reported strong correspondence with visual assessment and found that image-based quantification reduced subjective error and better resolved small differences at the low-severity end of the scale.

The significant genotype × treatment interaction shows that co-infection did not simply produce a uniformly larger version of the single-species response. Where co-infection increased disease, as in WBDC-237 and WBDC-175, *F. avenaceum* and *F. culmorum* may have added to, or enhanced, the damage caused by *F. graminearum*. The reduction in WBDC-110 and WBDC-164, the genotypes most damaged by *F. graminearum* alone, has two possible explanations that the present design cannot separate. First, because the total spore concentration was the same in both treatments, the Mix inoculum contained only about one third as many *F. graminearum* spores as the single-species inoculum; genotypes that are particularly susceptible to *F. graminearum* would be expected to show less disease if the other two species were less aggressive on them. Second, competition between species in the leaf tissue may have limited the growth of *F. graminearum*, which is consistent with the absence of FG16N amplification in co-infected samples discussed below. In either case, a genotype's response to *F. graminearum* alone did not reliably predict its response to co-infection, which supports including multi-species inoculations when screening for FHB resistance. The molecular analysis adds a further dimension to the phenotypic results. The FG16N assay, which is specific to *F. graminearum*, amplified in the single-species (Fg-only) samples but not in any co-infection (Mix) sample, in both WBDC-060 and WBDC-159. Because *F. graminearum* was part of the Mix inoculum, this is unlikely to reflect a true absence of the pathogen. Possible explanations are that *F. graminearum* was largely outcompeted by *F. avenaceum* and *F. culmorum* in the co-infected tissue; that its DNA was diluted within the mixed fungal template below the detection limit of end-point PCR, which is plausible given its lower starting dose in the Mix inoculum; or that the co-infected samples contained compounds that inhibited the PCR. These explanations cannot be distinguished with a qualitative (presence/absence) assay. Quantitative methods such as digital PCR (dPCR) or species-specific qPCR, together with an internal plant reference gene to check that the DNA can be amplified, would allow *F. graminearum* biomass to be compared directly between single-species and co-infection treatments.

The DON-type Tri13 assay gave the opposite pattern: amplification was detected in all co-infection samples of both genotypes, whereas *F. graminearum*-only samples were negative apart from one trace-level band in a WBDC-060 replicate, and the NIV-type primers did not amplify in any sample. Two points are important when interpreting this result. First, the assay detects a fungal gene in genomic DNA. It shows which trichothecene genotypes were present in the tissue, but not whether the biosynthesis pathway was active or how much toxin was produced; that would require gene-expression analysis (e.g. RT-qPCR) or chemical quantification of DON. Second, the Tri13 primers are not specific to *F. graminearum*: they were developed to determine the chemotype of *F. graminearum*, *F. culmorum* and *F. cerealis* (Chandler et al. 2003). The *F. culmorum* isolate in the Mix inoculum is therefore a likely source of the DON-type amplicon in the co-infected samples, which would also explain why the signal appeared in exactly the samples in which *F. graminearum* was not detected. The near-absence of a DON-type signal in *F. graminearum*-only samples is unexpected, because strain PH1 is a DON producer, and suggests that the Tri13 assay was less sensitive than the FG16N assay in this material. In wheat, co-inoculation of *F. graminearum* with other head blight species has been shown to change both the relative colonisation of each species and the amount of mycotoxin produced compared with single-species infection (Siou et al. 2015), and even weakly pathogenic members of the complex can alter disease and toxin outcomes. Changes in toxin production under co-infection are therefore plausible, but the present data cannot distinguish them from the simpler explanation that the DON-type signal came from *F. culmorum*. The absence of NIV-type amplification is consistent with the isolates used belonging to the DON chemotype, which predominates in many *F. graminearum* populations, whereas NIV production is more often associated with other species and particular geographic populations (Stępień et al. 2012).

The molecular pattern was the same in WBDC-060 and WBDC-159, even though these genotypes differed markedly in susceptibility in the phenotypic assays. This suggests that the treatment differences in FG16N and Tri13 detection reflect the composition of the fungal community in the leaf rather than genotype-specific host resistance. With only two genotypes and a small number of replicates, however, this needs to be tested on a larger panel.

4.1 Limitations

Several limitations should be considered while interpreting these results. The molecular assays were performed on a small number of biological replicates belonging to only two genotypes, so the patterns described above are to be treated as preliminary and hypothesis-generating, not conclusive. The PCR assays used

are end-point and qualitative, so they detect the presence of a target sequence rather than the quantity of fungal biomass or, in the case of the trichothecene genes, the amount of toxin actually produced; confirming real differences in DON accumulation between single and mixed species co-infection treatments would require a quantitative chemical method such as ELISA or LC-MS/MS, consistent with the mycotoxin quantification approaches reviewed by Stępień & Chełkowski (2010). Finally, the detached leaf assay, although a valuable and widely used pre-screening tool (Browne & Cooke, 2004, 2005; Rafiei et al., 2025), does not fully represent the whole-plant or field infection conditions. Mesterhazy et al. (2025) particularly cautions that resistance components identified under controlled, single-organ assays do not always directly translate into field-level resistance. Whole-plant architecture, flowering biology, and environmental exposure all influence natural infection in ways that a detached-leaf assay cannot fully capture. The identified resistance should therefore be validated under whole-plant and field conditions before it is used in a breeding programme. Further limitations concern the experimental design. First, the genotype rankings are based on a single screening experiment, and their reproducibility across independent experiments remains to be confirmed. Second, because the total spore concentration was kept at 1×10^6 spores mL^{-1} in both infection treatments, the Mix treatment combined two changes: the addition of *F. avenaceum* and *F. culmorum*, and a lower dose of *F. graminearum*. A design in which the additional species are added to a constant dose of *F. graminearum* would allow these effects to be separated.

4.2 Implications and future work

Taken together, the results of this study can be summarized in two main conclusions. First, several wild barley genotypes, most notably WBDC-060 and WBDC-034, showed consistent partial resistance to FHB with both phenotyping methods and merit further investigation as potential resistance donors. These results reinforce the case made by Fetch et al. (2003) and Steffenson et al. (2007) that wild barley collections such as the WBDC carry resistance diversity not yet captured in cultivated breeding pools. Using this diversity in breeding will require QTL mapping and marker-assisted selection, for which the genomic resources now available for wild barley (Spanner et al. 2026) provide a practical starting point. Second, co-infection with three *Fusarium* species changed disease relative to *F. graminearum* alone in a genotype-dependent way, and changed which fungal sequences could be detected in the leaf tissue. This is of practical relevance, since natural FHB infections in the field almost always involve more than one *Fusarium* species simultaneously (Lin et al., 2014; Tan et al., 2020), and resistance or toxin-risk assessments based purely on single-species inoculation cannot typically capture outcomes relevant with field conditions, a concern raised

by Mesterhazy et al. (2025) who argued that resistance screening protocols should better reflect the conditions that resistant germplasm will face in production. Future work should focus on prioritising: (i) quantifying *F. graminearum*, *F. culmorum* and *F. avenaceum* biomass by digital PCR or species-specific qPCR in single-species and co-infection samples, to test whether *F. graminearum* is outcompeted; (ii) quantifying DON by ELISA or LC-MS/MS to determine whether co-infection changes toxin accumulation, following approaches such as those used by Siou et al. (2015) in wheat; (iii) extending molecular assays to a wider panel of genotypes which covers the full spectrum of resistance as identified in the phenotypic screen; (iv) repeating the phenotypic screen with a design that keeps the *F. graminearum* dose constant between treatments; and (v) validating the most promising genotypes under whole-plant and field conditions.

5. Conclusions

The main conclusions of this study are:

(1) The detached leaf assay, combined with visual scoring and ImageJ-based lesion quantification, discriminated wild barley genotypes under both single-species and co-infection conditions, and the two scoring methods identified largely the same genotypes at the extremes of the susceptibility range.

(2) Co-infection with three *Fusarium* species increased disease relative to *F. graminearum* alone in most genotypes that responded differently to the two treatments, but reduced it in WBDC-110 and WBDC-164, the genotypes most susceptible to *F. graminearum* alone; the response to *F. graminearum* alone therefore did not always predict the response to co-infection.

(3) WBDC-060, WBDC-034 and WBDC-120 were the three least susceptible genotypes with both scoring methods, and WBDC-060 was the least susceptible overall; these accessions are candidates for further resistance characterisation.

(4) Co-infection altered the detectability of *F. graminearum* DNA and DON-associated Tri13 sequences in infected leaf tissue in both a partially resistant and a susceptible genotype. The DON-type signal under co-infection may come from *F. culmorum*; quantitative methods are needed to determine whether the pattern reflects competition between species and whether toxin production changes.

References

Ames, N., Dreiseitl, A., Steffenson, B.J. & Muehlbauer, G.J. (2015). Mining wild barley for powdery mildew resistance. *Plant Pathology*, 64 (6), 1396–1406. https://doi.org/10.1111/ppa.12384

Baek, S.G., Park, J.J., Kim, S., Lee, M.-J., Paek, J.-S., Choi, J., Jang, J.Y., Kim, J. & Lee, T. (2022). Evaluation of Barley and Wheat Germplasm for Resistance to Head Blight and Mycotoxin Production by Fusarium asiaticum and F. graminearum. *The Plant Pathology Journal*, 38 (6), 637–645. https://doi.org/10.5423/PPJ.OA.09.2022.0130

Browne, R.A. & Cooke, B.M. (2004). Development and Evaluation of an in vitro Detached Leaf Assay for Pre-Screening Resistance to Fusarium Head Blight in Wheat. *European Journal of Plant Pathology*, 110 (1), 91–102. https://doi.org/10.1023/B:EJPP.0000010143.20226.21

Browne, R.A. & Cooke, B.M. (2005). Resistance of wheat to Fusarium spp. in an in vitro seed germination assay and preliminary investigations into the relationship with Fusarium head blight resistance. *Euphytica*, 141 (1), 23–32. https://doi.org/10.1007/s10681-005-4820-0

Buerstmayr, H., Ban, T. & Anderson, J.A. (2009). QTL mapping and marker-assisted selection for Fusarium head blight resistance in wheat: a review. *Plant Breeding*, 128 (1), 1–26. https://doi.org/10.1111/j.1439-0523.2008.01550.x

Cappellini, R.A. & Peterson, J.L. (1965). Macroconidium Formation in Submerged Cultures by a Nonsporulating Strain of Gibberella Zeae. *Mycologia*, 57 (6), 962–966. https://doi.org/10.1080/00275514.1965.12018285

Chandler, E.A., Simpson, D.R., Thomsett, M.A. & Nicholson, P. (2003). Development of PCR assays to *Tri7* and *Tri13* trichothecene biosynthetic genes, and characterisation of chemotypes of *Fusarium graminearum*, *Fusarium culmorum* and *Fusarium cerealis*. *Physiological and Molecular Plant Pathology*, 62 (6), 355–367. https://doi.org/10.1016/S0885-5765(03)00092-4

Clear, R.M., Patrick, S.K., Gaba, D., Roscoe, M., Demeke, T., Pouleur, S., Couture, L., Ward, T.J., O'Donnell, K. & Turkington, T.K. (2006). Trichothecene and zearalenone production, in culture, by isolates of Fusarium pseudograminearum from western Canada. *Canadian Journal of Plant Pathology*, 28 (1), 131–136. https://doi.org/10.1080/07060660609507279

Dawson, I.K., Russell, J., Powell, W., Steffenson, B., Thomas, W.T.B. & Waugh, R. (2015). Barley: a translational model for adaptation to climate change. *New Phytologist*, 206 (3), 913–931. https://doi.org/10.1111/nph.13266

Dean, R., Van Kan, J. a. L., Pretorius, Z.A., Hammond-Kosack, K.E., Di Pietro, A., Spanu, P.D., Rudd, J.J., Dickman, M., Kahmann, R., Ellis, J. & Foster, G.D. (2012). The Top 10 fungal pathogens in molecular plant pathology. *Molecular Plant Pathology*, 13 (4), 414–430. https://doi.org/10.1111/j.1364-3703.2011.00783.x

Feng, C., Liu, H. & Tang, Z. (2018). Fusarium graminearum Inoculation on Wheat Head. *BIO-PROTOCOL*, 8 (15). https://doi.org/10.21769/BioProtoc.2964

Fernando, W.G.D., Oghenekaro, A.O., Tucker, J.R. & Badea, A. (2021). Building on a foundation: advances in epidemiology, resistance breeding, and forecasting research for reducing the impact of fusarium head blight in wheat and barley. *Canadian Journal of Plant Pathology*, 43 (4), 495–526. https://doi.org/10.1080/07060661.2020.1861102

Fetch, T.G., Steffenson, B.J. & Nevo, E. (2003). Diversity and Sources of Multiple Disease Resistance in Hordeum spontaneum. *Plant Disease*, 87 (12), 1439–1448. https://doi.org/10.1094/PDIS.2003.87.12.1439
Hoheneder, F., Biehl, E.M., Hofer, K., Petermeier, J., Groth, J., Herz, M., Rychlik, M., Heß, M. & Hückelhoven, R. (2022). Host Genotype and Weather Effects on Fusarium Head Blight Severity and Mycotoxin Load in Spring Barley. *Toxins*, 14 (2), 125. https://doi.org/10.3390/toxins14020125
Inglis, P.W., Pappas, M. de C.R., Resende, L.V. & Grattapaglia, D. (2018). Fast and inexpensive protocols for consistent extraction of high quality DNA and RNA from challenging plant and fungal samples for high-throughput SNP genotyping and sequencing applications. *PLOS ONE*, 13 (10), e0206085. https://doi.org/10.1371/journal.pone.0206085
Lin, Z., Xu, S., Que, Y., Wang, J., Comstock, J.C., Wei, J., McCord, P.H., Chen, B., Chen, R. & Zhang, M. (2014). Species-Specific Detection and Identification of Fusarium Species Complex, the Causal Agent of Sugarcane Pokkah Boeng in China. *PLOS ONE*, 9 (8), e104195. https://doi.org/10.1371/journal.pone.0104195
Linkmeyer, A., Götz, M., Hu, L., Asam, S., Rychlik, M., Hausladen, H., Hess, M. & Hückelhoven, R. (2013). Assessment and Introduction of Quantitative Resistance to Fusarium Head Blight in Elite Spring Barley. *Phytopathology*®, 103 (12), 1252–1259. https://doi.org/10.1094/PHYTO-02-13-0056-R
Ma, Z., Steffenson, B.J., Prom, L.K. & Lapitan, N.L.V. (2000). Mapping of Quantitative Trait Loci for Fusarium Head Blight Resistance in Barley. *Phytopathology*®, 90 (10), 1079–1088.
Madgwick, J.W., West, J.S., White, R.P., Semenov, M.A., Townsend, J.A., Turner, J.A. & Fitt, B.D.L. (2011). Impacts of climate change on wheat anthesis and fusarium ear blight in the UK. *European Journal of Plant Pathology*, 130 (1), 117–131. https://doi.org/10.1007/s10658-010-9739-1
Massman, J., Cooper, B., Horsley, R., Neate, S., Dill-Macky, R., Chao, S., Dong, Y., Schwarz, P., Muehlbauer, G.J. & Smith, K.P. (2011). Genome-wide association mapping of Fusarium head blight resistance in contemporary barley breeding germplasm. *Molecular Breeding*, 27 (4), 439–454. https://doi.org/10.1007/s11032-010-9442-0
McMullen, M., Bergstrom, G., De Wolf, E., Dill-Macky, R., Hershman, D., Shaner, G. & Van Sanford, D. (2012). A Unified Effort to Fight an Enemy of Wheat and Barley: Fusarium Head Blight. *Plant Disease*, 96 (12), 1712–1728. https://doi.org/10.1094/PDIS-03-12-0291-FE
Mesterhazy, A. (2020). Updating the Breeding Philosophy of Wheat to Fusarium Head Blight (FHB): Resistance Components, QTL Identification, and Phenotyping—A Review. *Plants*, 9 (12), 1702. https://doi.org/10.3390/plants9121702
Mesterhazy, Á., Tóth, B., Berényi, A., Ács, K. & Meszlényi, T. (2025). Significance of the Stability of Fusarium Head Blight Resistance in the Variety Registration, Breeding, and Genetic Research of Winter Wheat Using Disease Index, Fusarium-Damaged Kernels, and Deoxynivalenol Contamination. *Toxins*, 17 (6), 288. https://doi.org/10.3390/toxins17060288
Nganje, W.E., Bangsund, D.A., Leistritz, F.L., Wilson, W.W. & Tiapo, N.M. (2004). Regional Economic Impacts of Fusarium Head Blight in Wheat and Barley. *Applied Economic Perspectives and Policy*, 26 (3), 332–347. https://doi.org/10.1111/j.1467-9353.2004.00183.x
Nicholson, P., Simpson, D.R., Weston, G., Rezanoor, H.N., Lees, A.K., Parry, D.W. & Joyce, D. (1998). Detection and quantification of*Fusarium*

*culmorum*and*Fusarium graminearum*in cereals using PCR assays. *Physiological and Molecular Plant Pathology*, 53 (1), 17–37. https://doi.org/10.1006/pmpp.1998.0170
O'Donnell, K., Kistler, H.C., Tacke, B.K. & Casper, H.H. (2000). Gene genealogies reveal global phylogeographic structure and reproductive isolation among lineages of Fusarium graminearum, the fungus causing wheat scab. *Proceedings of the National Academy of Sciences*, 97 (14), 7905–7910. https://doi.org/10.1073/pnas.130193297
Parry, D.W., Jenkinson, P. & McLEOD, L. (1995). Fusarium ear blight (scab) in small grain cereals—a review. *Plant Pathology*, 44 (2), 207–238. https://doi.org/10.1111/j.1365-3059.1995.tb02773.x
Pereyra, S. & Dill-Macky, R. (2010). Fusarium Species Recovered from Wheat and Barley Grains in Uruguay, Pathogenicity and Deoxynivalenol Content. *Agrociencia Uruguay*, 14 (2), 33–44. https://doi.org/10.31285/AGRO.14.625
Perochon, A. & Doohan, F. (2016). Assessment of Wheat Resistance to Fusarium graminearum by Automated Image Analysis of Detached Leaves Assay. *BIO-PROTOCOL*, 6 (24). https://doi.org/10.21769/BioProtoc.2065
Rafiei, V., DeGenring, L., Schwister, E.M., Elmore, J.M., Dubey, M., Karlsson, M. & Drott, M.T. (2025). Comparative analysis of distinct phenotyping methods for assessing wheat resistance and pathogen virulence among Fusarium species causing head blight disease. *Plant Methods*, 21 (1), 85. https://doi.org/10.1186/s13007-025-01402-8
Roy, J.K., Smith, K.P., Muehlbauer, G.J., Chao, S., Close, T.J. & Steffenson, B.J. (2010). Association mapping of spot blotch resistance in wild barley. *Molecular Breeding*, 26 (2), 243–256. https://doi.org/10.1007/s11032-010-9402-8
Sato, K., Flavell, A., Russell, J., Börner, A. & Valkoun, J. (2014). Genetic Diversity and Germplasm Management: Wild Barley, Landraces, Breeding Materials. In: Kumlehn, J. & Stein, N. (eds) *Biotechnological Approaches to Barley Improvement*. Springer. 21–36. https://doi.org/10.1007/978-3-662-44406-1_2
Schneider, C.A., Rasband, W.S. & Eliceiri, K.W. (2012). NIH Image to ImageJ: 25 years of image analysis. *Nature Methods*, 9 (7), 671–675. https://doi.org/10.1038/nmeth.2089
Siou, D., Gélisse, S., Laval, V., Elbelt, S., Repinçay, C., Bourdat-Deschamps, M., Suffert, F. & Lannou, C. (2015). Interactions between Head Blight Pathogens: Consequences for Disease Development and Toxin Production in Wheat Spikes. *Applied and Environmental Microbiology*, 81 (3), 957–965. https://doi.org/10.1128/AEM.02879-14
Spanner, R., Sallam, A.H., Guo, Y., Jayakodi, M., Himmelbach, A., Fiebig, A., Simmons, J., Bethke, G., Lee, Y., Pacheco Arge, L.W., Qiu, Y., Badea, A., Baum, M., Belzile, F., Ben-David, R., Brueggeman, R., Case, A., Cattivelli, L., Davis, M., Dockter, C., Doležel, J., Dreiseitl, A., Gavin, R., Glick, L., Greiner, S., Hamilton, R., Hayes, P.M., Heisel, S., Henson, C., Kilian, B., Komatsuda, T., Li, C., Liu, C., Mahalingam, R., Maruschewski, M., Matny, O., Maurer, A., Mayer, K.F.X., Mayrose, I., Moscou, M., Muehlbauer, G.J., Oono, Y., Ordon, F., Özkan, H., Pecinka, A., Perovic, D., Pillen, K., Pourkheirandish, M., Russell, J., Šafář, J., Salvi, S., Sanchez-Garcia, M., Sato, K., Schmutzer, T., Scholz, U., Scott, J., Singh Brar, G., Smith, K.P., Sorrells, M.E., Spannagl, M., Stein, N., Tondelli, A., Tuberosa, R., Tucker, J., Turkington, T., Valkoun, J., Verma, R.P.S., Vinje, M.A., von Korff, M., Walling, J.G., Waugh, R., Wise, R.P., Wulff, B.B.H., Yang, S., Zhang, G., Morrell, P.L., Mascher, M. & Steffenson, B.J. (2026). Whole-genome resequencing of the wild barley diversity

collection: a resource for identifying and exploiting genetic variation for cultivated barley improvement. *G3 Genes|Genomes|Genetics*, 16 (1), jkaf261. https://doi.org/10.1093/g3journal/jkaf261
Stanisz, E., Zgoła-Grześkowiak, A., Waśkiewicz, A., Stępień, Ł. & Beszterda, M. (2015). Can Ergosterol Be an Indicator of *Fusarium* Fungi and Mycotoxins in Cereal Products? *Journal of the Brazilian Chemical Society*, 26, 705–712. https://doi.org/https://doi.org/10.5935/0103-5053.20150030
Steffenson, B.J., Olivera, P., Roy, J.K., Jin, Y., Smith, K.P. & Muehlbauer, G.J. (2007). A walk on the wild side: mining wild wheat and barley collections for rust resistance genes. *Australian Journal of Agricultural Research*, 58 (6), 532–544. https://doi.org/10.1071/AR07123
Steiner, B., Kurz, H., Lemmens, M. & Buerstmayr, H. (2009). Differential gene expression of related wheat lines with contrasting levels of head blight resistance after Fusarium graminearum inoculation. *Theoretical and Applied Genetics*, 118 (4), 753–764. https://doi.org/10.1007/s00122-008-0935-8
Stępień, Ł. & Chełkowski, J. (2010). Fusarium head blight of wheat: pathogenic species and their mycotoxins. *World Mycotoxin Journal*, 3 (2), 107–119. https://doi.org/10.3920/WMJ2009.1193
Stępień, Ł., Gromadzka, K. & Chełkowski, J. (2012). Polymorphism of mycotoxin biosynthetic genes among Fusarium equiseti isolates from Italy and Poland. *Journal of Applied Genetics*, 53 (2), 227–236. https://doi.org/10.1007/s13353-012-0085-1
Tan, J., Ameye, M., Landschoot, S., De Zutter, N., De Saeger, S., De Boevre, M., Abdallah, M.F., Van der Lee, T., Waalwijk, C. & Audenaert, K. (2020). At the scene of the crime: New insights into the role of weakly pathogenic members of the fusarium head blight disease complex. *Molecular Plant Pathology*, 21 (12), 1559–1572. https://doi.org/10.1111/mpp.12996
Trail, F. (2009). For Blighted Waves of Grain: Fusarium graminearum in the Postgenomics Era. *Plant Physiology*, 149 (1), 103–110. https://doi.org/10.1104/pp.108.129684
Xu, X.-M., Monger, W., Ritieni, A. & Nicholson, P. (2007). Effect of temperature and duration of wetness during initial infection periods on disease development, fungal biomass and mycotoxin concentrations on wheat inoculated with single, or combinations of, Fusarium species. *Plant Pathology*, 56 (6), 943–956. https://doi.org/10.1111/j.1365-3059.2007.01650.x
Zhou, M.X. (2010). Barley Production and Consumption. In: Zhang, G. & Li, C. (eds) *Genetics and Improvement of Barley Malt Quality*. Springer. 1–17. https://doi.org/10.1007/978-3-642-01279-2_1

Popular science summary

Barley is one of the world's most important cereal crops, used for animal feed, malting and food. A fungal disease called Fusarium head blight attacks barley and wheat, reducing yields and contaminating the grain with toxins that make it unsafe for people and animals. The disease is caused not by one fungus but by a group of related *Fusarium* species that often attack the same plant at the same time. Spraying fungicides only partly controls it, so plant breeders are looking for barley plants that are naturally resistant. Modern barley has lost much of its genetic diversity during domestication and breeding. Its wild ancestor, wild barley, still grows in the Middle East and Central Asia and carries a much wider range of genes, including genes for disease resistance. In this project, I tested 40 wild barley types from an international collection to see how they respond to *Fusarium* fungi, both when infected by one species and when infected by three species together.

Instead of growing every plant until it flowers, which takes months, I used a quick laboratory test: leaves were cut from young plants, placed on agar in Petri dishes and infected with fungal spores. After five days, I measured the size of the dead patches on the leaves, both by eye using a scoring scale and by measuring them precisely on photographs with computer software. The two methods identified largely the same resistant and susceptible types. Some wild barley types, especially one called WBDC-060, developed only small patches, while others were severely affected. Interestingly, infection with three species together did not always make things worse: some plants that resisted one fungus well became more diseased when all three were present, while the most susceptible plants were less affected.

I also used DNA tests on two of the plants and found that the presence of several fungi changed which fungi could be detected in the leaves. This suggests that the fungi compete with each other inside the leaf. The most promising wild barley types now need to be tested on whole plants in the field. In the long run, they could help breeders develop barley varieties that are better protected against this damaging disease.

Acknowledgements

I would like to thank my supervisor, Vahidehalsadat Rafieebanadaki, and my assistant supervisors, Fredrik Dolfors and Magnus Karlsson, for their guidance and support throughout this project. I also thank Prof. Brian Steffenson, University of Minnesota, for providing the seed of the Wild Barley Diversity Collection. I am also thankful to Anna Berlin for her valuable comments as examiner, and the staff of the Department of Forest Mycology and Plant Pathology for their help in the laboratory and phytotron.

Appendix 1

Wild barley accessions from the Wild Barley Diversity Collection (WBDC) used in this study, with their ICARDA genebank (IG) numbers and countries of origin.

Table A1. Wild barley accessions used in this study (n = 40)

Accession	IG number	Country of origin
WBDC-005	38616	Jordan
WBDC-009	38633	Jordan
WBDC-010	38653	Afghanistan
WBDC-012	38656	Afghanistan
WBDC-018	38670	Afghanistan
WBDC-025	38693	Pakistan
WBDC-034	38912	Palestine
WBDC-038	39117	Palestine
WBDC-060	39891	Egypt
WBDC-070	39932	Syria
WBDC-109	40090	Syria
WBDC-110	40091	Syria
WBDC-117	40106	Turkmenistan
WBDC-120	40109	Tajikistan
WBDC-121	40138	Iran
WBDC-122	40140	Iran
WBDC-123	40142	Iran
WBDC-134	40179	Lebanon
WBDC-159	110739	Syria
WBDC-160	110742	Syria
WBDC-164	110773	Syria
WBDC-167	110804	Syria
WBDC-172	112673	Iran
WBDC-175	112680	Iran
WBDC-221	131674	Tajikistan
WBDC-223	131684	Tajikistan
WBDC-231	132636	Azerbaijan
WBDC-233	38668	Afghanistan
WBDC-237	40033	Jordan
WBDC-244	135700	Jordan

WBDC-245	38621	Jordan
WBDC-248	39394	Jordan
WBDC-250	39988	Jordan
WBDC-253	115787	Jordan
WBDC-254	115790	Jordan
WBDC-296	135336	Syria
WBDC-298	135357	Syria
WBDC-300	117896	Syria
WBDC-304	40161	Syria
WBDC-306	40166	Syria

Publishing and archiving

Approved students' theses at SLU can be published online. As a student you own the copyright to your work and in such cases, you need to approve the publication. In connection with your approval of publication, SLU will process your personal data (name) to make the work searchable on the internet. You can revoke your consent at any time by contacting the library.

Even if you choose not to publish the work or if you revoke your approval, the thesis will be archived digitally according to archive legislation.

You will find links to SLU's publication agreement and SLU's processing of personal data and your rights on this page:

- https://libanswers.slu.se/en/faq/228318

☒ YES, I, Mohsin Bashir Khan, have read and agree to the agreement for publication and the personal data processing that takes place in connection with this.